

Energy and Electron Transfer in Photosystem II of a Chlorophyll *b*-Containing *Synechocystis* sp. PCC 6803 Mutant[†]

Dmitrii Vavilin,^{†,§} Hong Xu,^{†,§} Su Lin,^{§,||} and Wim Vermaas^{*,†,§}

Department of Plant Biology, Department of Chemistry and Biochemistry, and
Center for the Studies of Early Events in Photosynthesis, Arizona State University, Tempe, Arizona 85287

Received September 13, 2002; Revised Manuscript Received December 19, 2002

ABSTRACT: Using a *Synechocystis* sp. PCC 6803 mutant strain that lacks photosystem (PS) I and that synthesizes chlorophyll (Chl) *b*, a pigment that is not naturally present in the wild-type cyanobacterium, the functional consequences of incorporation of this pigment into the PS II core complex were investigated. Despite substitution of up to 75% of the Chl *a* in the PS II core complex by Chl *b*, the modified PS II centers remained essentially functional and were able to oxidize water and reduce Q_A, even upon selective excitation of Chl *b* at 460 nm. Time-resolved fluorescence decay measurements upon Chl excitation showed a significant reduction in the amplitude of the 60–70 ps component of fluorescence decay in open Chl *b*-containing PS II centers. This may indicate slower energy transfer from the PS II core antenna to the reaction center pigments or slower energy trapping. Chl *b* and pheophytin *b* were present in isolated PS II reaction centers. Pheophytin *b* can be reversibly photoreduced, as evidenced from the absorption bleaching at ~440 and 650 nm upon illumination in the presence of dithionite. Upon excitation at 685 nm, transient absorption measurements using PS II particles showed some bleaching at 650 nm together with a major decrease in absorption around 678 nm. The 650 nm bleaching that developed within ~10 ps after the flash and then remained virtually unchanged for up to 1 ns was attributed to formation of reduced pheophytin *b* and oxidized Chl *b* in some PS II reaction centers. Chl *b*-containing PS II had a lower rate of charge recombination of Q_A^{•-} with the donor side and a significantly decreased yield of delayed luminescence in the presence of DCMU. Taken together, the data suggest that Chl *b* and pheophytin *b* participate in electron-transfer reactions in PS II reaction centers of Chl *b*-containing mutant of *Synechocystis* without significant impairment of PS II function.

Photosystem II (PS II)¹ is a multisubunit pigment–protein complex that is a part of the photosynthetic apparatus in plants and cyanobacteria and that uses light energy to catalyze reduction of plastoquinone by water (for recent

reviews see refs 1–3). The proteins that are key to PS II function include the reaction center proteins D1 and D2, the chlorophyll-binding proteins CP43 and CP47, the α and β subunits of cytochrome *b*₅₅₉, and the Mn-stabilizing protein of the oxygen-evolving complex.

The D1 and D2 proteins carry redox components involved in electron-transfer reactions in PS II. Light energy absorbed by light-harvesting pigment molecules migrates to the reaction center and causes charge separation between the primary electron donor P680, consisting of presumably several chlorophyll *a* molecules, and the primary electron acceptor pheophytin *a* (reviewed in refs 3–5). To stabilize the charge separation, the electron is transferred from pheophytin to the primary electron-accepting plastoquinone Q_A and then to the plastoquinone pool through the exchangeable plastoquinone Q_B. The highly oxidizing potential of P680⁺ drives donor-side oxidation of Tyr_Z (Tyr161 of D1), which subsequently withdraws an electron from the Mn-containing oxygen-evolving complex. Other redox-active components of the PS II reaction center, such as Tyr_D (Tyr160 of D2), a carotenoid, a chlorophyll (Chl_Z), and cytochrome *b*₅₅₉, are also able to donate electrons to P680⁺, although with lower quantum yield (6).

The structure of the PS II complex from the thermophilic cyanobacterium *Thermosynechococcus elongatus* has been

[†] This research was supported by a grant from the Department of Energy to W.V. (DE-FG03-95ER20180).

* Corresponding author. Tel: (480) 965-3698. Fax: (480) 965-6899. E-mail: wim@asu.edu.

[‡] Department of Plant Biology, Box 871601.

[§] Center for the Studies of Early Events in Photosynthesis.

^{||} Department of Chemistry and Biochemistry, Box 871604.

¹ Abbreviations: B_A, monomeric accessory chlorophyll on the active (D1) branch of the PS II reaction center; B_B, monomeric accessory chlorophyll on the inactive (D2) branch of the PS II reaction center; Chl_D, chlorophyll_D, a peripheral chlorophyll in the PS II reaction center; Chl_Z, chlorophyll_Z, a peripheral chlorophyll in the PS II reaction center serving as an accessory electron donor in PS II; DCMU, 3-(3,4-dichlorophenyl)-1,1-dimethylurea; DMBQ, 2,5-dimethyl-*p*-benzoquinone; E_m, midpoint redox potential; F_M, maximal fluorescence; F_o, constant fluorescence; F_V, variable fluorescence; HPLC, high-performance liquid chromatography; LHC, light-harvesting complex; MES, 2-(*N*-morpholino)ethanesulfonic acid; Pheo, pheophytin; PS I, photosystem I; PS II, photosystem II; P680, primary electron donor in PS II; P_A, a chlorophyll in the reaction center coordinated by D1-His198; P_B, a chlorophyll in the reaction center coordinated by D2-His197; Q_A, the primary electron-accepting quinone in PS II; Q_B, the secondary electron accepting quinone in PS II; TES, *N*-tris(hydroxymethyl)methyl-2-aminoethanesulfonic acid; Tyr_D, D2-Tyr160, an accessory electron donor in PS II; Tyr_Z, D1-Tyr161, the physiological electron donor to P680.

determined by X-ray crystallography at 3.8 Å resolution (7). The crystallography data show 26 chlorophylls ligated to the CP43 and CP47 proteins and 2 pheophytins and 6 chlorophylls associated with the D1 and D2 proteins of the reaction center. The 2 pheophytins and 4 chlorophylls (out of 6) in the PS II reaction center are arranged in two nearly C_2 symmetrical branches, similar to that found in reaction centers of purple nonsulfur bacteria. Therefore, these four chlorophylls of the PS II reaction center are sometimes labeled as P_A , P_B , B_A , and B_B (see refs 3, 8, and 9), i.e., in the same way as reaction center pigments of bacterial systems. Indexes A and B indicate active and inactive branches of electron transfer, respectively. The other two chlorophylls associated with D1 and D2 proteins (Chl_z and Chl_D , respectively) are located at the periphery of the PS II reaction center and have no homologues in the bacterial reaction center.

In bacterial reaction centers, the P_A and P_B molecules form a strongly coupled dimer (special pair). Upon primary charge separation, the P_A/P_B pair donates an electron to bacterio-pheophytin, apparently via the accessory bacteriochlorophyll B_A (10). In contrast, coupling between the homologous "special pair" chlorophylls P_A and P_B in PS II is much weaker (11), probably because of the greater spatial separation of the two molecules (~ 10 Å center to center (7)). It was proposed that at ≤ 80 K primary charge separation in PS II occurs exclusively from the excited B_A chlorophyll, with subsequent stabilization of the positive charge primarily on P_A (9). At room temperature charge separation may also be initiated from molecule(s) other than B_A (9; but see ref 5) with subsequent formation of the $P680^+Pheo^-$ state, in which the positive charge (hole) is delocalized among several chlorophyll species constituting the P680 site (4, 5, 9).

Normally the D1, D2, CP43, and CP47 proteins bind only "a"-type porphyrins, i.e., chlorophyll *a* and pheophytin *a*. The CP43 and CP47 proteins function as an inner antenna system that is connected to a secondary light-harvesting system. In higher plants, selected algae, and prochlorophytes this secondary light-harvesting system contains chlorophyll *a* and chlorophyll *b* molecules. In contrast, phycobilisomes serve as the secondary light-harvesting system in cyanobacteria. Cyanobacteria cannot synthesize chlorophyll *b* and do not have LHC (light-harvesting complex) proteins typical for the secondary light-harvesting antenna complex in plants. We have created a PS I-less mutant of the cyanobacterium *Synechocystis* sp. PCC 6803 that is able to synthesize large amounts of chlorophyll *b* (12). In this mutant the *cao* and *lhcb* genes from a higher plant that encode chlorophyll *a* oxidase (the enzyme that converts chlorophyll *a* into chlorophyll *b*) and a major chlorophyll *a/b* binding LHC protein associated with PS II (LHCII), respectively, were incorporated into the genome of *Synechocystis* and expressed under strong native promoters. The LHCII protein apparently degrades rapidly in this mutant, and the synthesized chlorophyll *b* replaced the majority of chlorophyll *a* in PS II (12).

In this work, we characterize PS II properties of this chlorophyll *b*-containing PS II complex. Biochemical and spectroscopic analysis suggests that chlorophyll *b* can occupy most of the chlorophyll *a*-binding sites associated with CP43 and CP47 and several chlorophyll binding sites associated with the D1 and D2 proteins.

MATERIALS AND METHODS

Strains and Growth Conditions. Construction and growth conditions of two *Synechocystis* sp. PCC 6803 strains, the PS I-less/*chlL*⁻ (parental) and PS I-less/*chlL*⁻/*lhcb*⁺/*cao*⁺ (*lhcb*⁺/*cao*⁺) strains have been described previously (12). The growth temperature, which impacts the chlorophyll *a/b* ratio of the *lhcb*⁺/*cao*⁺ strain, varied from 28 to 37 °C.

Isolation of Thylakoid Membranes and PS II Particles. Thylakoid membranes and PS II core particles were prepared essentially using the protocol of Tang and Diner (13) with some modifications. To avoid pheophytinization of chlorophyll, all media were buffered with 50 mM TES–NaOH at pH = 7.4 instead of MES–NaOH (pH = 6.0). Considering that in our study PS II core particles were isolated from PS I-less cells, which have a 5-fold reduced chlorophyll content (14), initial solubilization of thylakoid membranes in dodecyl maltoside was performed at a lower chlorophyll concentration (0.1 mg/mL) compared to at 1 mg/mL used by Tang and Diner (13). The final concentration of the detergent was 0.4% (w/v), and the extraction proceeded in the dark for 40 min. The suspension was then centrifuged at 30 000 rpm in a Beckman 50.2Ti rotor for 30 min at 4 °C, and the obtained supernatant was loaded onto a DEAE-Toyopearl 650S column (3 × 11 cm) previously equilibrated with a buffer containing 5 mM MgCl₂, 10 mM CaCl₂, 50 mM TES–NaOH (pH = 7.4), 20% (v/v) glycerol, and 0.03% (w/v) dodecyl maltoside. The column was washed with equilibration buffer (500 mL) at a flow rate of 5 mL/min. Then 500 mL of a linear gradient from 0 to 35 mM MgSO₄ in equilibration buffer was applied to the column with fractions being collected from the beginning of the gradient. The first fractions containing phycobilins and PS II particles enriched with carotenoids were discarded, and the later fractions containing purified PS II core particles were collected for further usage.

Isolation of PS II Reaction Centers. PS II reaction centers from *Synechocystis* cells were prepared essentially by method of Giorgi and coauthors (15). Initial solubilization of PS I-less thylakoid membranes in 4.5% (w/v) Triton X-100 was performed at a lower chlorophyll concentration (90 μg of chlorophyll mL⁻¹) compared to at 450 μg of chlorophyll mL⁻¹ used for PS I-containing thylakoids in ref 16. PS II reaction center preparations from PS I-less *Synechocystis* cells contained a substantial amount of contaminating cytochromes presumably because of the higher cytochrome *b₆f* content of the starting material. The abundance of cytochromes precluded the use of cytochrome *b₅₅₉* for quantification of PS II reaction centers.

Pigment Analysis. Pigments from whole cells were extracted with methanol supplemented with 0.01% (v/v) ammonium hydroxide, and the extracts were analyzed by HPLC (12) or spectrophotometrically using extinction coefficients provided by Lichtenthaler (16). Extraction of pigments from PS II core particles or from reaction center preparations was performed with acetone supplemented with 0.01% (v/v) ammonium hydroxide; three volumes of the sample were added to seven volumes of acetone. Insoluble material was removed by centrifugation, the pigments were reextracted from the supernatant with hexane, concentrated, if necessary, under a stream of nitrogen gas, and then subjected to HPLC analysis. The pigments were detected at

654 nm (pheophytin *b*), 646 nm (chlorophyll *b*), and at 665 nm (chlorophyll *a* and pheophytin *a*). Standards used were chlorophyll *b* purchased from Sigma, chlorophyll *a* isolated from wild-type *Synechocystis* cells, and pheophytin *a* and pheophytin *b* obtained by acidification of 1 mL of acetone solution of the corresponding chlorophyll with 1 μ L of concentrated HCl. The extinction coefficients for chlorophyll *a* (76.79 mM⁻¹ cm⁻¹ at 663.6 nm) and chlorophyll *b* (47.04 mM⁻¹ cm⁻¹ at 646.6 nm) in 80% acetone were taken from Porra and coauthors (17).

Fluorescence Emission Spectra. Fluorescence emission spectra were recorded upon excitation of cell suspensions or isolated thylakoids (chlorophyll concentration 0.8–1.2 μ g mL⁻¹) by monochromatic light using a FluoroMax spectrofluorometer (Spex Industries, Inc). To measure room-temperature fluorescence emission spectra of *Synechocystis* cells with PS II centers open, the culture was pumped through a flow-through cuvette at a rate of 5 mL s⁻¹. A 5 μ M concentration of DCMU (an inhibitor that blocks electron transfer from Q_A to Q_B) was added to the culture, and the pumping was stopped to record the fluorescence emission spectra with PS II centers closed. Fluorescence at 77 K was measured as described in ref 12. To remove phycobilisomes from the thylakoid preparation, the thylakoid suspension was washed several times with a buffer containing 50 mM MES–NaOH (pH = 6.5) and 20 mM sodium pyrophosphate before the fluorescence measurement. Gaussian analysis of the fluorescence emission spectra was performed using Origin 6.0 software (Microcal Software Inc.).

Fluorescence Induction. Fluorescence induction was recorded with a FluoroMax spectrofluorometer (see ref 12 for details). A 5 μ M concentration of DCMU and 1 mM NH₂OH were added to the cells in complete darkness 1 min before the room-temperature measurements. NH₂OH functionally replaces the Mn cluster of the oxygen-evolving complex thereby preventing charge recombination of Q_A⁻ with the donor side. In the presence of both DCMU and NH₂OH, PS II can be excited at a very low light intensity to monitor fluorescence induction without charge recombination-induced artifacts, thus overcoming the limited time resolution of the spectrofluorometer.

Delayed Luminescence. Kinetics of delayed luminescence were recorded using a FluoroMax spectrofluorometer equipped with a temperature-controlled cuvette holder after excitation of DCMU-treated (5 mM) intact cells with a saturating single-turnover Xe flash. Luminescence was detected at 680 nm (the bandwidth at half-maximum was 16 nm). The recording of the delayed luminescence signal was started 10 ms after the flash and continued for up to 5 s. The value of the integral under the curve was taken to characterize intensity of delayed luminescence.

Variable Fluorescence Decay. The decay of variable fluorescence was detected with a PAM fluorometer (Walz, Effeltrich, Germany) as described previously (18). Every trace was recorded using a fresh sample. The measurements were repeated 5 times at each temperature, and the averaged curve was used for further analysis of decay components.

Time-Resolved Fluorescence Decay Kinetics. Time-resolved fluorescence of intact cells of *Synechocystis* was measured at room temperature in a single-photon-timing spectrometer as described by Bittersmann and Vermaas (19). Phycobilins were excited at 600 nm using a cavity-dumped

dye laser system, synchronously pumped by a Nd:YAG laser (Coherent Antares). The half-width of the output pulses was 5–15 ps at a repetition rate of 4 MHz with a mean power of less than 5 mW on the sample. Chlorophylls were excited at 432 or 455 nm by a Tsunami mode-locked Ti:sapphire laser equipped with a model 3980 frequency doubler/pulse selection unit and continuously pumped by a Millennia diode-Nd:YVO₄ laser (Spectra Physics). The \sim 2 ps excitation pulses were delivered at a frequency of 4.2 MHz. Emission was detected through a monochromator with bandwidths set at 8 (excitation at 432 or 600 nm) or 16 nm (excitation at 455 nm). The full width at half-maximum of the instrument response function determined by measuring light scattering from *Synechocystis* cells was 75 to 150 ps depending on the excitation wavelength.

Transient Absorption Spectroscopy. Measurements of transient absorption spectra of the PS II core particles were performed at room temperature using a femtosecond laser spectrometer described earlier (20). A small amount of K₃-Fe(CN)₆ (1 mol of ferricyanide/mol of PS II) was added to PS II core particles to oxidize Q_A in all reaction centers, and the sample was loaded into an optical wheel with a 2 mm path length that was rotating with a frequency of 2–4 Hz to ensure excitation of a fresh sample with every laser pulse. The pump laser pulses (\sim 150 fs duration) centered at 685 nm excited samples at a frequency of 1 kHz. The intensity of the pump pulses was low enough to avoid singlet–singlet annihilation of excitations in PS II.

Oxygen Evolution. O₂ evolution was measured at 25 °C with a Hansatech oxygen electrode (Hansatech, King's Lynn, England) as described in ref 12. Actinic light provided by a KL 1500 illuminator (Walz, Effeltrich, Germany) was passed through a long-wave-pass filter transmitting light with a wavelength longer than 560 nm before reaching the sample. When predominantly chlorophyll excitation was desired, the light was filtered through a LS-500 short-wave-pass filter (Corion) that transmits light with a wavelength shorter than 500 nm. The light intensity was adjusted with a set of neutral density filters (Corion).

Pheophytin Photoreduction. PS II core preparations were diluted to a final chlorophyll concentration of 3.4 μ M with a buffer containing 50 mM TES–NaOH (pH 7.8), 5 mM MgCl₂, 5 mM CaCl₂, 20% glycerol, 0.03% dodecyl maltoside (w/v), 0.23 mg/mL glucose oxidase, 80 μ g/mL catalase, and 10 mM glucose (the last three chemicals were used to create anaerobic conditions). Samples were transferred to a cuvette (1 cm optical path length) and incubated in darkness with 3 mM sodium dithionite and 1 μ M methyl viologen for 2 min; they were subsequently illuminated for 40 s with red or blue light (\sim 1000 μ mol of photons m⁻² s⁻¹) from the side of the cuvette to photoaccumulate reduced pheophytin. Absorption spectra of the samples were determined using a computer-controlled Cary 5 spectrophotometer (Varian). The absorption spectrum was first recorded during the last 10 s of illumination (the light spectrum). After the actinic light was turned off, the spectrum was recorded 4 times at 30 s intervals. In contrast to PS II core particles obtained from the parental PS I-less/*chlL*⁻ strain, the chlorophyll *b*-containing preparation appeared to be rather unstable in the presence of dithionite; a gradual bleaching at 648 nm accompanied by appearance of a 665 nm peak (presumably due to a chemical modification of chlorophyll *b*) developed in these samples

Table 1: Chlorophyll and Pheophytin Composition^a

strain	sample	Chl <i>a</i>	Chl <i>b</i>	Pheo <i>a</i>	Pheo <i>b</i>	Chl (<i>a</i> + <i>b</i>) / 2 Pheo (<i>a</i> + <i>b</i>)
PS I-less/ <i>chlL</i> [−] (parental)	whole cells	38.5 ± 0.3	0.0	2.0 ± 0.1	0.0	38.5 ± 0.5
	PS II core particles	37.3 ± 0.3	0.0	2.0 ± 0.1	0.0	37.3 ± 0.5
	PS II reaction centers	7.8 ± 0.2	0.0	2.0 ± 0.1	0.0	7.8 ± 0.3
PS I-less/ <i>chlL</i> [−] / <i>lhcb</i> ⁺ / <i>cao</i> ⁺	whole cells	13.5 ± 0.1	24.6 ± 0.2	0.8 ± 0.1	1.2 ± 0.1	38.1 ± 0.4
	PS II core particles (early fraction)	12.3 ± 0.1	26.8 ± 0.3	0.8 ± 0.1	1.2 ± 0.1	39.1 ± 0.6
	PS II core particles (late fraction)	14.3 ± 0.1	22.9 ± 0.2	1.0 ± 0.1	1.0 ± 0.1	37.2 ± 0.3
	PS II reaction centers	5.7 ± 0.1	4.6 ± 0.1	1.8 ± 0.1	0.2 ± 0.05	10.3 ± 0.2

^a The composition of chlorophyll and pheophytin was determined in whole cells of the PS I-less/*chlL*[−] parental strain and the *lhcb*⁺/*cao*⁺ mutant and in PS II core particles (D1/D2/CP47/CP43/cyt *b*₅₅₉) and PS II reaction center preparations (D1/D2/cyt *b*₅₅₉) obtained from these cells. The pigment composition was determined by HPLC and was normalized to two pheophytins (*a* + *b*). Shown are average values ±SD for three pigment determinations.

even in the absence of illumination. To correct the absorption changes due to photoaccumulation of reduced pheophytin for the dithionite-induced light-independent pigment modifications, the changes in absorption during the dark incubation period that followed the illumination were linearly extrapolated to a zero time-point corresponding to the moment when the light spectrum was taken. The difference spectrum characterizing solely pheophytin photoreduction was obtained by subtracting the extrapolated dark spectrum from the light one. This correction is justified because reoxidation of pheophytin in the control sample is essentially completed during the first 30 s of dark incubation, whereas light-independent changes typical for the chlorophyll *b*-containing PS II core preparation continue for many minutes with apparently zero-order kinetics at a relatively slow rate.

RESULTS

Pigment Composition of Intact Cells and Isolated PS II Core Particles. The PS I-less/*chlL*[−] parental strain lacks chlorophyll *b*, as expected, but the *lhcb*⁺/*cao*⁺ strain derived therefrom synthesized a significant amount of chlorophyll *b*; the chlorophyll *b/a* ratio in the *lhcb*⁺/*cao*⁺ strain depended significantly on growth temperature and varied from 1.2 at 28 °C to 3.1 at 37 °C. Another pigment detected exclusively in the *lhcb*⁺/*cao*⁺ strain was pheophytin *b*. Table 1 compares the chlorophyll and pheophytin content in the PS I-less/*chlL*[−] parental strain and in the *lhcb*⁺/*cao*⁺ mutant grown at 30 °C. Under these conditions, the chlorophyll *b/a* ratio in the *lhcb*⁺/*cao*⁺ mutant varied from 1.6 to 2.0. The PS I-less/*chlL*[−] parental strain contained about 38 chlorophyll *a* molecules/2 pheophytin *a*. The same chlorophyll-to-pheophytin ratio was obtained for the *lhcb*⁺/*cao*⁺ mutant if both types of chlorophyll and pheophytin (*a* and *b*) were taken into account.

PS II core particles isolated from the PS I-less/*chlL*[−] strain by column chromatography contained about 37 chlorophyll *a*/2 pheophytin *a* molecules. This result is in excellent agreement with the earlier estimation of the chlorophyll-to-pheophytin ratio of 37.5 in PS II particles isolated from wild-type *Synechocystis* sp. PCC 6803 after correction for a small contamination with PS I (13). As expected, PS II core complexes isolated from the *lhcb*⁺/*cao*⁺ mutant contained chlorophyll *b* and pheophytin *b* together with the typical *a*-type pigments. However, this preparation appeared to be rather heterogeneous: fractions of PS II particles that eluted early from the column were enriched in chlorophyll *b* and pheophytin *b* as compared to later eluting fractions. The total

chlorophyll-to-pheophytin ratio in the late fractions was the same as in PS II cores isolated from the parental PS I-less/*chlL*[−] cells. In early fractions this ratio was a little higher than in extracts from whole cells (see Table 1). This may be due to contamination of the early fractions with potential chlorophyll-binding proteins such as SCPs (21) that are not components of the PS II core.

Interestingly, when isolation of PS II core particles from PS I-less *Synechocystis* cells (both the parental strain and *lhcb*⁺/*cao*⁺ mutant) was performed in a buffer at pH = 6.0 (rather than at pH = 7.4; Table 1), the measured chlorophyll to 2 pheophytin ratio was reduced to 32–33 (data not shown). This is very close to the value of 34 chlorophyll molecules/2 pheophytins reported for a preparation of PS II core particles isolated from a *Synechocystis* mutant with a His-tagged CP47 polypeptide (22). Considering that in the latter case the isolation was also performed at pH = 6.0, it is likely that even slight acidification of the isolation medium leads to pheophytinization of some chlorophyll, although the lower pH is best for stabilizing an active oxygen evolving complex (see, for example, ref 13).

Pigment Composition of Isolated PS II Reaction Centers. Because of the abundance of chlorophyll *b* in *lhcb*⁺/*cao*⁺ cells and because of the apparently limited specificity of pigment-binding sites in PS II for the type of chlorophyll bound (12) chlorophyll *b* may occupy chlorophyll *a*-binding sites not only in the CP43 and CP47 antenna proteins but also in the PS II reaction center itself. To test this, we isolated PS II reaction centers (D1/D2/cytochrome *b*₅₅₉ pigment–protein complexes) from the *lhcb*⁺/*cao*⁺ mutant and compared the pigment composition of this preparation with that isolated from the PS I-less/*chlL*[−] parental strain. HPLC analysis confirmed the presence of chlorophyll *b* in PS II reaction centers isolated from the *lhcb*⁺/*cao*⁺ mutant, but the amount of pheophytin *b* in this preparation was very low and the chlorophyll-to-pheophytin ratio was higher than in the PS I-less/*chlL*[−] strain (Table 1). A possible explanation for the low pheophytin *b* content and the high chlorophyll-to-pheophytin ratio in the reaction center preparation from the *lhcb*⁺/*cao*⁺ mutant is that pheophytin *b* that is present in PS II core particles, presumably in reaction centers (Table 1), is washed out easily, for example because it is bound less tightly than pheophytin *a*.

Spectral Properties of Isolated PS II Reaction Centers. For better resolution of the absorption properties of PS II reaction centers, the absorption spectrum was recorded at 77 K. As expected, a large contribution of chlorophyll *b* (a

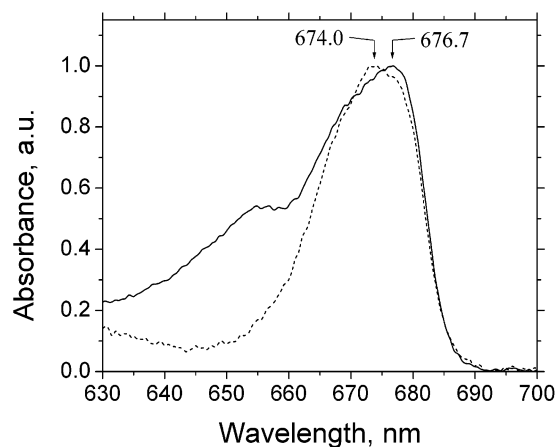


FIGURE 1: 77 K absorption spectra of PS II reaction center preparations. PS II reaction centers were isolated from the *lhcb*⁺/*cao*⁺ mutant (—) and from the PS I-less/*chlL*[−] parental strain (---). The spectra were recorded between 630 and 700 nm, corresponding to the Q_y region of chlorophylls, and normalized to the absorption maximum.

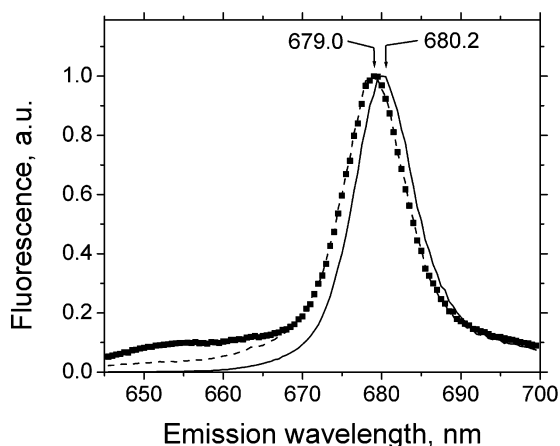


FIGURE 2: 77 K fluorescence emission spectra of PS II reaction center preparations. PS II reaction centers were isolated from the *lhcb*⁺/*cao*⁺ mutant (—, ■) and from the parental PS I-less/*chlL*[−] strain (---, —). Samples were excited at 435 (---, —) or at 465 (—, ■) nm.

wide shoulder around 640–660 nm) was apparent in spectra of PS II reaction centers isolated from the *lhcb*⁺/*cao*⁺ strain (Figure 1). Moreover, the spectrum of the chlorophyll *b*-containing reaction centers exhibited a red shift of the absorption maximum from 674 to 677 nm as compared to the control reaction centers, suggestive of a preferential replacement of short-wavelength chlorophyll(s) absorbing around 674 nm by chlorophyll *b*. In contrast to the red-shifted absorption maximum, the 77 K fluorescence emission spectrum of chlorophyll *b*-containing reaction centers was slightly blue-shifted relative to the control (679 versus 680.2 nm, Figure 2). The width of the fluorescence emission band remained almost identical in reaction centers from both strains. The change in the fluorescence emission maximum suggests that, in addition to some of the short-wavelength chlorophyll(s), the most red-absorbing pigments in the parental strain may also have been replaced by chlorophyll *b* in the *lhcb*⁺/*cao*⁺ mutant. Another interesting feature of reaction centers from the *lhcb*⁺/*cao*⁺ strain is that only a small fluorescence emission shoulder around 653 nm appeared upon excitation at 460 nm (exciting chlorophyll *b*), whereas the shape of the major fluorescence emission band

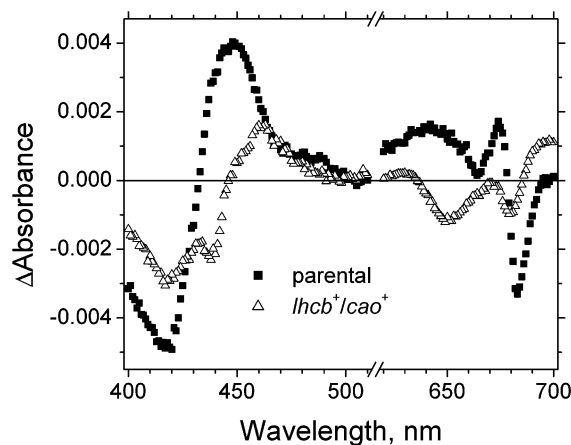


FIGURE 3: Absorption difference spectra associated with photoaccumulation of reduced pheophytin. Photoinduced (light-minus-dark) changes in the absorption spectra of *Synechocystis* PS II core particles isolated from the parental PS I-less/*chlL*[−] strain (■) and from the *lhcb*⁺/*cao*⁺ mutant (△) were measured in the presence of 3 mM sodium dithionite and 1 μM methyl viologen. The light-minus-dark difference spectra of both types of samples were corrected for dithionite-induced light-independent absorption changes as described in Materials and Methods although the light-independent changes were minor in PS II core particles isolated from the parental strain. The chlorophyll concentration was ~3.4 μM. The chlorophyll *b/a* ratio in PS II cores isolated from the *lhcb*⁺/*cao*⁺ mutant was 1.6. The measurements of difference spectra in the blue light region were performed upon excitation of the samples with light filtered through a red filter ($\lambda \geq 625$ nm), and corresponding measurements in the red region of the spectrum were performed upon excitation of the samples with blue light ($\lambda \leq 500$ nm). The excitation light intensity was 1000 μmol of photons m^{−2} s^{−1} in both spectral regions.

at 679 nm did not change (Figure 2). Consequently, the majority of chlorophyll *b* molecules in the PS II reaction center preparations are functionally coupled to chlorophyll *a*.

Pheophytin Reduction. To verify that pheophytin *b* is present in intact PS II reaction centers and to determine whether this pigment (rather than pheophytin *a*) might participate in electron-transfer reactions, we measured photoinduced absorption changes in isolated PS II core particles in the presence of dithionite and methyl viologen, conditions that favor photoaccumulation of reduced pheophytin (23). The light-minus-dark difference spectrum of PS II core particles isolated from the PS I-less/*chlL*[−] parental strain showed minima around 418 and 682 nm and a maximum at 450 nm (Figure 3), in line with what would be expected from pheophytin *a* reduction. In preparations from the *lhcb*⁺/*cao*⁺ mutant an additional minimum at 440 nm appeared in the blue region of the difference spectrum, whereas the maximum at 450 nm typical for PS II core particles from the parental strain was shifted to 460 nm. In the red region of the difference spectrum, in PS II core particles of the *lhcb*⁺/*cao*⁺ mutant a new broad band appeared with a minimum around 650 nm. The 682 nm minimum greatly decreased in amplitude and shifted to slightly shorter wavelength (~679 nm), which may be due to an increase in the relative contribution of an electrochromic shift in a 679 nm chlorophyll absorption band (8).

Figure 3 suggests that the amount of pheophytin *a* reduction is greatly decreased in the *lhcb*⁺/*cao*⁺ core particles and that a component absorbing at 440 and 650 nm is

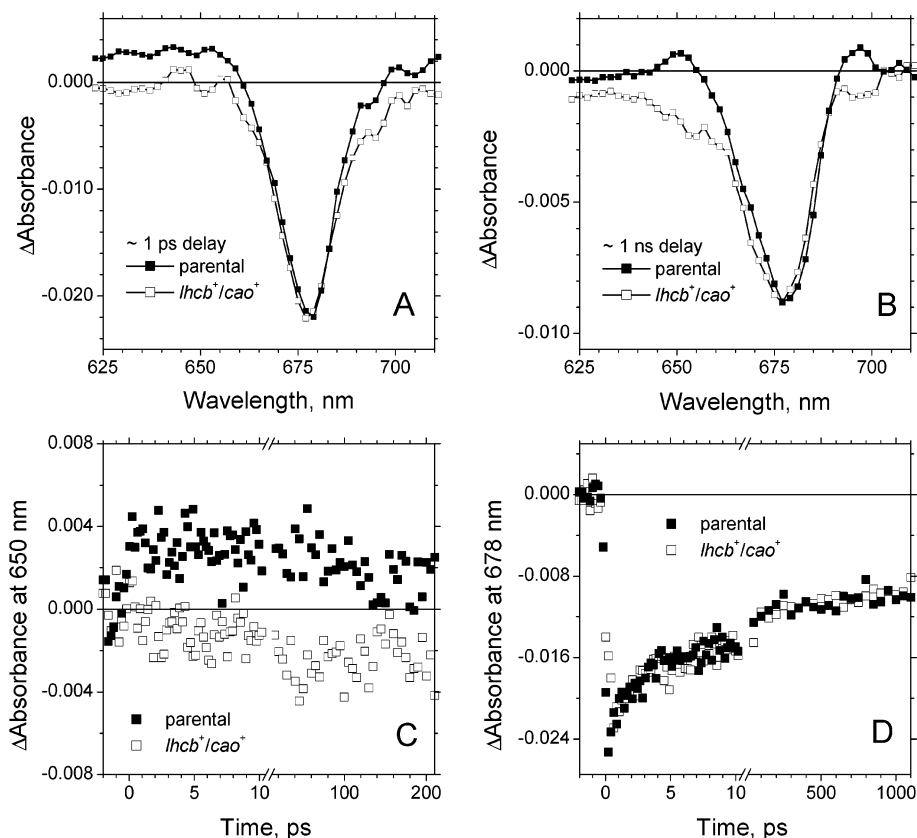


FIGURE 4: Transient changes in absorption of photosystem II core particles isolated from the *lhcb⁺/cao⁺* (□) and the parental PS I[−] less/*chlL[−]* (■) strains of *Synechocystis* upon excitation with 685 nm pump pulses. Shown are transient absorption spectra at 1 ps (A) and 1 ns (B) pump–probe delay and corresponding kinetics of absorption changes at 650 nm (C) and 678 nm (D).

bleached. We assign this component to be pheophytin *b*. Pheophytin reduction is accompanied by bleaching around the Soret and *Q_y* absorption bands (see refs 23 and 24), which for pheophytin *a* in PS II are centered at about 420 and 680 nm, respectively. In organic solvents, the Soret absorption maximum of pheophytin *b* is shifted to longer wavelength by $\sim 19 \pm 6$ nm relative to pheophytin *a*, whereas the *Q_y* band is shifted to shorter wavelength by $\sim 7 \pm 6$ nm compared to pheophytin *a* (16). Considering that the protein environment modifies the position of the absorption maxima of the pigments, we assign the spectral bleaching at 440 and 650 nm in the PS II core preparation from the *lhcb⁺/cao⁺* mutant to the photoaccumulation of pheophytin *b*. This, along with the decreased bleaching at 418 nm and at about 680 nm in PS II core particles from the *lhcb⁺/cao⁺* mutant, suggests that a major part of the photoreducible pheophytin *a* has been substituted by pheophytin *b* in the mutant.

Transient Absorption Spectra of PS II Cores. As nearly half of the chlorophyll in reaction centers from the *lhcb⁺/cao⁺* mutant is chlorophyll *b* (Table 1), the possible involvement of chlorophyll *b* in primary electron-transfer reactions in *lhcb⁺/cao⁺* PS II was analyzed. Transient absorption spectra of isolated core particles were recorded at different time delays after excitation with a pump laser pulse centered at 685 nm; light at this wavelength is absorbed predominantly by long-wavelength *a*-type pigments of the PS II reaction center. Figure 4 A,B shows differential absorption profiles recorded in PS II core preparations from the parental and *lhcb⁺/cao⁺* strains 1 ps and 1 ns after the excitation pulse. The spectra of both types of PS II core particles were characterized by a pronounced bleaching at

~ 678 nm, which decayed in time with apparently the same multiphasic kinetics in chlorophyll *b*-containing and control PS II core preparations (Figure 4D). The decay of the bleaching at 678 nm in both preparations can be reasonably well approximated with two decay components ($\tau = 7\text{--}9$ ps and $\tau = 80\text{--}120$ ps) and a nondecaying part. In addition to the major 678 nm bleaching band, the transient absorption spectra of chlorophyll *b*-containing PS II core preparations recorded 1 ns after the excitation pulse had developed some bleaching around 650 nm (Figure 4B). In contrast, a small increase in absorption at 650 nm was observed after 1 ns in PS II particles from the parental strain. As shown in Figure 4C, the increase in 650 nm absorption in core particles of the parental strain developed essentially at the time of the actinic pulse, whereas the build in of the bleaching in *lhcb⁺/cao⁺* particles was much slower (half-time of about 10 ps). Once developed, the intensity of bleaching at 650 nm remained unchanged for up to 1 ns. This suggests that upon excitation of *a*-type pigments some bleaching of a *b*-type pigment is induced.

Variable Fluorescence and Delayed Luminescence: Temperature Dependence. Where possible, intact cells were used to compare functional properties of chlorophyll *b*-containing and control PS II complexes to minimize potential artifacts. By measurement of decay kinetics of variable fluorescence (F_v) after exposure of DCMU-treated cells to a 200 ms flash of light, the rate of Q_A^- recombination with the donor side in PS II of the *lhcb⁺/cao⁺* mutant was compared to that of the parental PS I-less/*chlL[−]* strain. The decay kinetics in both mutants can be fitted by a sum of two exponentials with approximately equal amplitudes of fast and slow phases of

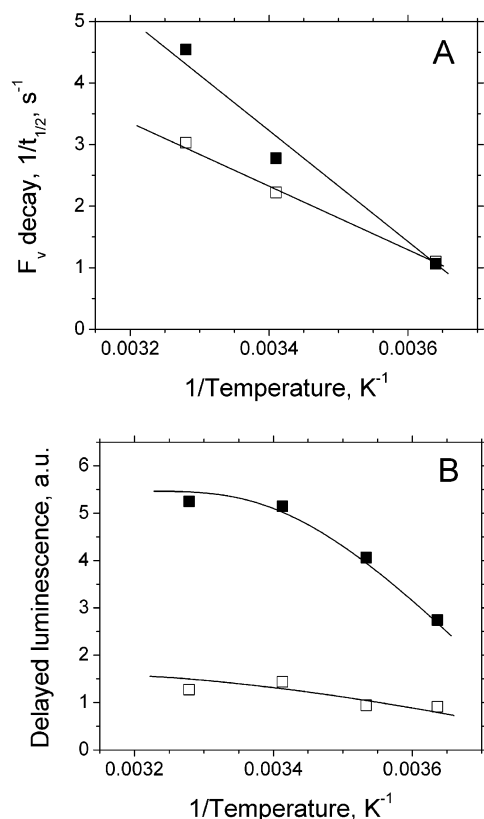


FIGURE 5: Temperature dependence of the half-time of F_v decay (A) and the intensity of delayed luminescence (B) in intact cells of the *lhcb*⁺/*cao*⁺ mutant (□) and of the PS I-less/*chlL*⁻ parental strain (■). To all cell suspensions, DCMU was added to a final concentration of 5 μ M. To measure F_v decay, cells were incubated for 3 min at a given temperature in darkness and were then illuminated by a 200 ms pulse of red light (30 μ mol of photons $m^{-2} s^{-1}$). Subsequently, changes in F_v were monitored after termination of the pulse. The half-time of F_v decay was determined after averaging five decay curves, each curve recorded with a fresh sample. To measure delayed luminescence, cells (1.6 μ g of chlorophyll/mL) were incubated for 3 min at given temperature in darkness and were then exposed to a saturating single-turnover Xe flash. The delayed luminescence signal was recorded for 5 s starting 10 ms after the flash. The value of the integral under the curve was calculated to determine intensity of delayed luminescence. The chlorophyll *b/a* ratio in the *lhcb*⁺/*cao*⁺ cells was 1.8.

decay (data not shown, but see ref 18 for decay traces in the control PS I-less strain). The overall half-time of F_v decay was taken as a parameter to compare Q_A^- stability in the two strains at temperatures from +2 to 32 °C. Figure 5 A shows that Q_A^- decayed somewhat slower in chlorophyll *b*-containing PS II. The difference in F_v decay rates between the two strains was larger at higher temperatures indicating that the apparent activation energy of Q_A^- decay is lower in the *lhcb*⁺/*cao*⁺ strain.

The kinetics of delayed luminescence emitted upon recombination of Q_A^- with the donor side after excitation of PS II with a saturating flash were slower in *lhcb*⁺/*cao*⁺ cells compared to PS I-less/*chlL*⁻ cells and accelerated at higher temperatures in both strains (data not shown). The integral intensity of delayed luminescence was about 4-fold lower in the *lhcb*⁺/*cao*⁺ mutant relative to the parental chlorophyll *b*-less cells at all temperatures (Figure 5 B). The delayed luminescence was measured upon excitation of PS II with saturating flashes. Samples from the two types of cells contained an equal amount of chlorophyll, and the

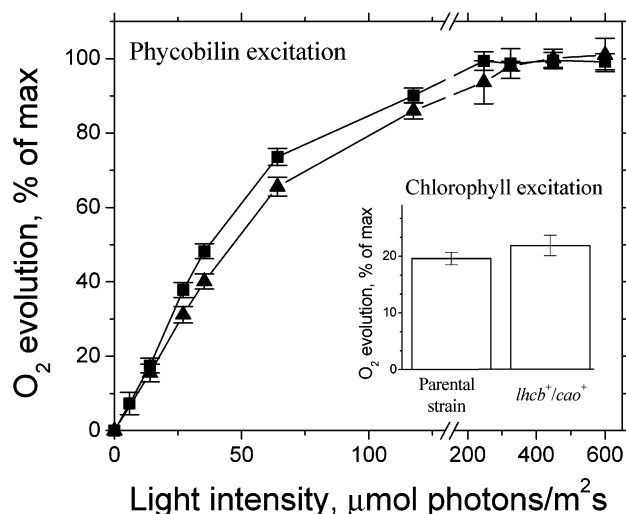


FIGURE 6: Light-response curves of oxygen evolution. Oxygen evolution was measured in intact cells of the *lhcb*⁺/*cao*⁺ mutant (▲) and of the PS I-less/*chlL*⁻ parental strain (■) upon excitation of predominantly phycobilins at $\lambda \geq 560$ nm. The maximum oxygen evolution rate at saturating light intensity was 1600 μ mol of O_2 /(mg of Chl·h) for the *lhcb*⁺/*cao*⁺ mutant and 2100 μ mol of O_2 /(mg of Chl·h) for the PS I-less/*chlL*⁻ strain. The 0.2 mM DMBQ and 1 mM $K_3Fe(CN)_6$ were added to the cells as electron acceptors. The inset compares rates of oxygen evolution in the two strains upon predominant chlorophyll excitation at $\lambda \leq 500$ nm at a limiting light intensity of 200 μ mol of photons $m^{-2} s^{-1}$. The chlorophyll *b/a* ratio in the *lhcb*⁺/*cao*⁺ cells was 2.9. Each data point represents an average \pm SD of three experiments.

concentration of functional PS II centers was similar in both samples (see ref 12). Consequently, the results obtained indicate that the efficiency of formation of excited chlorophyll upon charge recombination of Q_A^- with the donor side in chlorophyll *b*-containing PS II is significantly reduced, as compared to in the control strain.

Oxygen Evolution. The rate of oxygen evolution measured in intact cells of the *lhcb*⁺/*cao*⁺ strain at saturating light intensity was 70–80% of the value measured in the PS I-less/*chlL*⁻ parental strain. Figure 6 shows normalized light saturation curves of oxygen evolution in the two strains upon excitation with $\lambda \geq 560$ nm light that is absorbed mostly by phycobilins. For the chlorophyll *b*-containing *lhcb*⁺/*cao*⁺ mutant, about 20% more light was required to half-saturate oxygen evolution, as compared to the PS I-less/*chlL*⁻ strain. Largely, this difference may be due to the fact that on a per cell (OD₇₃₀) basis the *lhcb*⁺/*cao*⁺ mutant contained about 15% less phycobilins than the parental PS I-less/*chlL*⁻ strain (data not shown). When oxygen evolution at limiting light intensity was recorded in the two strains upon predominant excitation of chlorophylls with blue light ($\lambda \leq 500$ nm), the *lhcb*⁺/*cao*⁺ mutant had a 10% higher rate of O_2 evolution than the parental PS I-less/*chlL*⁻ strain, in line with a broader spectrum of light utilization in the chlorophyll *b*-containing strain. Taken together these results suggest that chlorophyll *b*-containing PS II complexes capable of oxygen evolution have a photosynthetic efficiency that is similar to that of PS II complexes that contain only chlorophyll *a*.

Fluorescence Induction. Measurements of fluorescence induction in the presence of DCMU and NH_2OH provide a way to estimate changes in the overall efficiency of PS II complexes upon modification of their pigment composition. In this experiment, cells were excited with weak monochro-

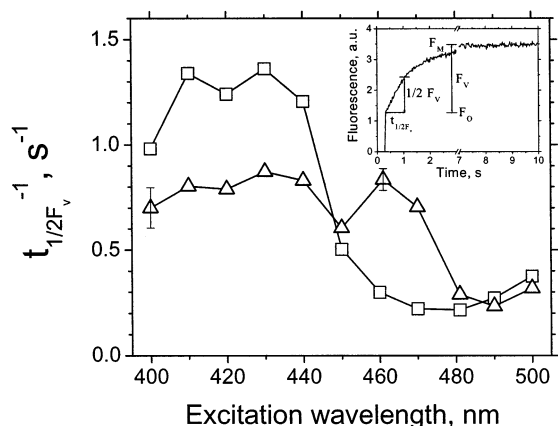


FIGURE 7: Wavelength dependence of the Q_A reduction rate in PS II of the *lhcb⁺/cao⁺* mutant (Δ) and the PS I-less/*chlL⁻* parental strain (\square). The rates of Q_A reduction upon excitation of intact cells with monochromatic light at different wavelengths were compared on the basis of $1/t_{1/2F_v}$ values. $t_{1/2F_v}$ was calculated from the fluorescence induction curves measured in the presence of 1 mM NH_2OH and 5 μM DCMU for each excitation wavelength as shown in the inset. The chlorophyll *b/a* ratio in the *lhcb⁺/cao⁺* cells was 1.4.

matic light (light intensity of less than 1 $\mu\text{mol photons m}^{-2} \text{ s}^{-1}$) at different wavelengths, and the time $t_{1/2F_v}$ required for the variable fluorescence F_v to reach half of the maximum value was determined (see the inset to Figure 7). Figure 7 shows the wavelength dependence of the $1/t_{1/2F_v}$ values characterizing the rate of Q_A reduction in the *lhcb⁺/cao⁺* mutant and in the PS I-less/*chlL⁻* parental strain. In contrast to the parental strain, light absorbed by chlorophyll *b* at 460–470 nm in the *lhcb⁺/cao⁺* cells is about as efficient in Q_A reduction as light absorbed by chlorophyll *a* at 430 nm. The total amount of chlorophyll molecules appears to be the same in PS II complexes from the *cao⁺/lhcb⁺* and the PS I-less/*chlL⁻* cells (Table 1). Therefore, assuming that the absorption cross section of PS II integrated from 400 to 480 nm is similar in the two strains, one can compare the efficiency of Q_A reduction in the chlorophyll *b*-containing and parental PS II cells by integrating the obtained $1/t_{1/2F_v}$ values plotted in Figure 7 over the wavelength range from 400 to 480 nm. This calculation suggests that the energy absorbed by PS II centers from the *lhcb⁺/cao⁺* mutant leads to Q_A^- formation with 85–90% efficiency as compared to normal chlorophyll *a*-containing PS II. Considering that phycobilins contribute to some extent to the absorption in the blue spectral region and that the phycobilin amount is somewhat reduced in the *lhcb⁺/cao⁺* strain, the difference in the quantum yield leading to stable charge separation in the two types of PS II complexes is expected to be even less than 10–15%. As will be shown in the next paragraphs, part of this difference can be attributed to the reduced efficiency of energy transfer from PS II core/phycobilisome complex to the reaction center in chlorophyll *b*-containing PS II.

Fluorescence Emission Spectra. To monitor energy transfer in intact PS II, room-temperature fluorescence emission spectra were recorded in *Synechocystis* cells with different chlorophyll *b/a* ratios. As expected, upon chlorophyll *a* excitation at 435 nm, the fluorescence emission spectrum of the PS I-less/*chlL⁻* strain showed a fluorescence emission peak at 680 nm and a small shoulder at 650–670 nm (Figure 8 A). Upon reduction of Q_A , the intensity of the fluorescence

emission increased by a factor of 3, but the spectrum remained qualitatively the same. The fluorescence emission within the 630–685 nm spectral window was fitted with a sum of three Gaussian components that correspond to the fluorescence from the phycobilisome terminal emitter(s) and chlorophyll *a* in PS II ($\lambda_{\text{max}} = 680.8$ nm), allophycocyanin ($\lambda_{\text{max}} = 665.0$ nm), and phycocyanin ($\lambda_{\text{max}} = 640.1$ nm). The emission intensity of the 680.8 nm component dominated in the chlorophyll *b*-less strain.

In chlorophyll *b*-containing cells, the relative contribution of the 650–670 nm shoulder to overall fluorescence increased with increasing chlorophyll *b* content (Figure 8B,C), whereas the increase in the fluorescence intensity upon closure of PS II centers became less prominent. The fluorescence emission spectra of chlorophyll *b*-containing cells can be fitted essentially with the same set of components that was used for the analysis of fluorescence in the parental strain. However, the best fit was obtained when the emission maximum corresponding to allophycocyanin was shifted from 665.0 to 662.8 and 662.4 nm in the *lhcb⁺/cao⁺* cultures with chlorophyll *b/a* ratio of 1.4 and 3.1, respectively. The relative intensity of the 662.4–662.8 nm fluorescence bands was much stronger in chlorophyll *b*-containing cells than in the parental strain.

The Q_y band absorption of protein-associated chlorophyll *b* generally peaks at 645–660 nm (25); therefore, both chlorophyll *b* and phycobilisomes can contribute to the intensive fluorescence emission at 650–670 nm in the *lhcb⁺/cao⁺* mutant. In fact, a small blue shift in the fluorescence emission maximum of the 662–665 nm Gaussian component, observed in *lhcb⁺/cao⁺* cells, might be assigned to a contribution of chlorophyll *b* fluorescence, which is expected to peak at slightly shorter wavelength than allophycocyanin. To determine the origin of the 650–670 nm fluorescence, the fluorescence spectrum emitted by intact cells of the *lhcb⁺/cao⁺* mutant with PS II centers closed was compared with the fluorescence emission spectrum of thylakoids, which were isolated from these cells and which were essentially depleted of phycobilisomes during the isolation (see Materials and Methods for details). As phycobilisome removal greatly reduced the intensity of the 650–670 nm shoulder (Figure 9), this emission in the *lhcb⁺/cao⁺* strain originated predominantly from phycobilins. Excitation of thylakoid fluorescence at 460 nm, a wavelength at which chlorophyll *b* absorption is maximal but phycobilins absorb less than at 435 nm, caused a further decrease in fluorescence emission at 650–660 nm. Therefore, if chlorophyll *b* contributes to a small extent to the 650–670 nm fluorescence shoulder, this emission is expected to be associated with chlorophyll *b* that is excitonically connected to other PS II pigments rather than with free chlorophyll *b*.

Time-Resolved Fluorescence: Excitation at 600 nm. To study the influence of the presence of chlorophyll *b* on excitation energy transfer between phycobilisomes and the PS II complex in more detail, fluorescence decay kinetics were measured in intact cells of the *lhcb⁺/cao⁺* mutant and of the parental PS I-less/*chlL⁻* strain. The decay of fluorescence elicited by selective laser-pulse excitation of phycobilin pigments at 600 nm was recorded in the wavelength region from 620 to 700 nm at 10 nm intervals. Global analysis of the fluorescence data in the entire region was performed, and the results are shown in Figure 10. The fit quality was

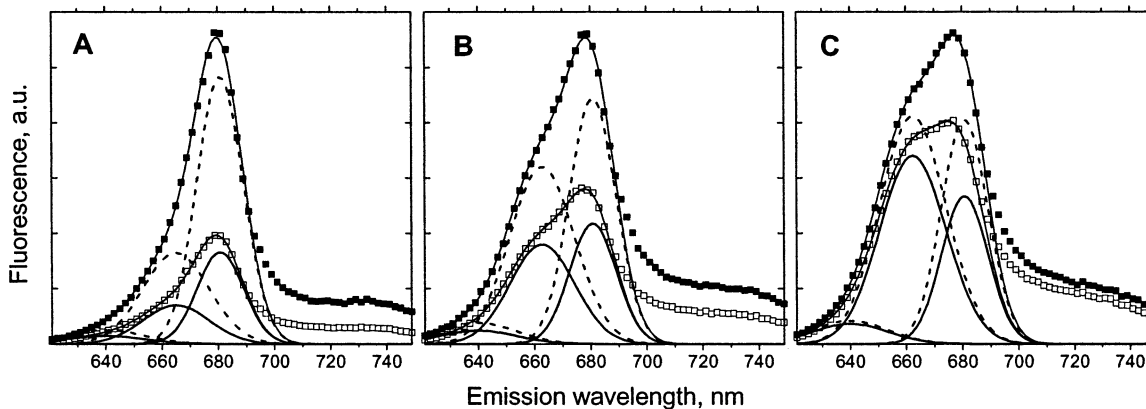


FIGURE 8: Gaussian analysis of room-temperature fluorescence emission spectra of intact cells. Fluorescence was measured in intact cells of the parental PS I-less/*chlL*[−] strain (A) and of the *lhcb*⁺/*cao*⁺ (B, C) mutant with PS II centers open (□) or closed (■). Excitation was at 436 nm. The chlorophyll *b/a* ratio in the *cao*⁺/*lhcb*⁺ cells was 1.4 (B) and 3.1 (C). The spectra of each culture were normalized to the corresponding F_m value. Fluorescence data between 620 and 685 nm were fitted with three Gaussian components shown by thick solid (F_m) or dashed (F_m) lines; thin lines indicate the sum of the corresponding components. The widths at half-maximum of the Gaussian components were set equal to 19.2 nm (λ_{\max} = 680.8 nm), 27.8 nm (λ_{\max} = 665, 662.8, and 662.4 nm in panels A–C, respectively), and 31.6 nm (λ_{\max} = 640.1 nm).

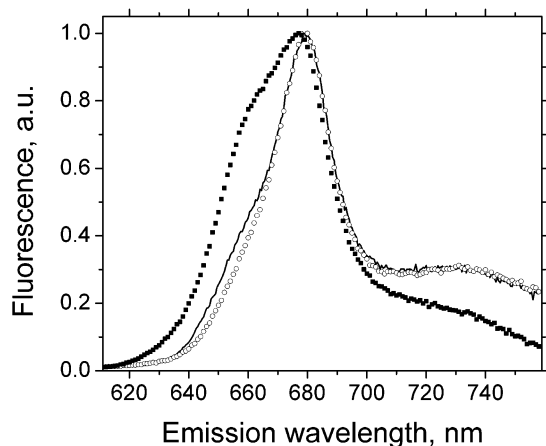


FIGURE 9: Room-temperature fluorescence emission spectra of intact *lhcb*⁺/*cao*⁺ cells (■) and of phycobilin-free thylakoids isolated from these cells (○). Excitation was at 435 nm (—, ■) or at 460 nm (---, ○). The chlorophyll *b/a* ratio in the cells and in thylakoids was 3.1.

evaluated by its global χ^2 value and weighted residual plots (data not shown). For both strains five lifetime components were sufficient for a good fit.

The decay-associated fluorescence spectrum of the PS I-less/*chlL*[−] strain contained two short-lived components (τ = 24–27 ps and τ = 160–170 ps) with fluorescence maxima around 640 and 650–660 nm, representing phycobilisome components. The decay time of these short-lived components was not affected by reduction state of Q_A in PS II. Judging from their spectral characteristics, the 24–27 ps component may be due to fluorescence of phycocyanin transferring energy to allophycocyanin, whereas the 160–170 ps component may represent the excited allophycocyanin transferring energy to the terminal emitter and to chlorophyll *a* in the PS II core. The other three components with lifetimes ranging from 300 ps to 3.5 ns peaked at 680 nm. This wavelength corresponds to emission from chlorophyll *a* and from the terminal emitter of phycobilisomes. In cells with open PS II centers (dark-adapted, no DCMU added), the main components of fluorescence peaking at 680 nm decayed with lifetimes τ = 400 ps and τ = 1.36 ns; the amplitude of the τ = 400 ps component dominated. When the PS II centers

were closed in the PS I-less/*chlL*[−] strain, the two 680 nm components became slightly slower (τ increasing to 480 ps and 1.48 ns, respectively), whereas their relative amplitudes increased considerably, as expected from the considerable variable fluorescence in this strain (see Figure 8A).

In the *lhcb*⁺/*cao*⁺ mutant, the lifetimes of the two fastest components of fluorescence decay (associated with energy transfer within phycobilisomes; peak maxima at 640 and 650–660 nm) were virtually identical to the lifetimes of the corresponding components in the parental PS I-less/*chlL*[−] strain. One of the major differences between the two strains was a significant broadening of the slower components ($\tau \geq 370$ ps), which were shifted to the blue by about 10 nm in the *lhcb*⁺/*cao*⁺ strain. This suggests the involvement of multiple pigments in the fluorescence decays with $\tau \geq 370$ ps in chlorophyll *b*-containing PS II complexes. Taking into account that chlorophyll *b* does not contribute considerably to the fluorescence in the *lhcb*⁺/*cao*⁺ mutant (see Figure 9), the components with τ = 370–390 ps and τ = 1.28–1.31 ns are likely to reflect reactions taking place in PS II with the excitation equilibrated between PS II chlorophylls, terminal emitter(s) of phycobilisomes, and allophycocyanin; the equilibrium is substantially shifted toward excited allophycocyanin in the presence of chlorophyll *b* in PS II.

The slowest component of the fluorescence decay ($\tau \sim 3.5$ ns) with an emission maximum at about 680 nm had very small relative amplitude in both the PS I-less/*chlL*[−] parental strain and in the *cao*⁺/*lhcb*⁺ mutant. This component is often assigned to emission from excitonically disconnected pigments (26). However, an increase in the amplitude of the 3.5 ns emission observed upon the closure of PS II centers suggests contribution of PS II pigments to this slowly decaying fluorescence emission component.

Time-Resolved Fluorescence: Excitation at 435 nm. To investigate energy transfer and trapping in chlorophyll *b*-containing reaction centers, fluorescence decay kinetics in whole cells were recorded upon predominant excitation of chlorophyll *a* at 435 nm. In this experiment, we were especially interested in short-lived components of fluorescence decay ($\tau \sim 25$ –100 ps), which reflect a composite of excitation energy transfer and primary charge separation in

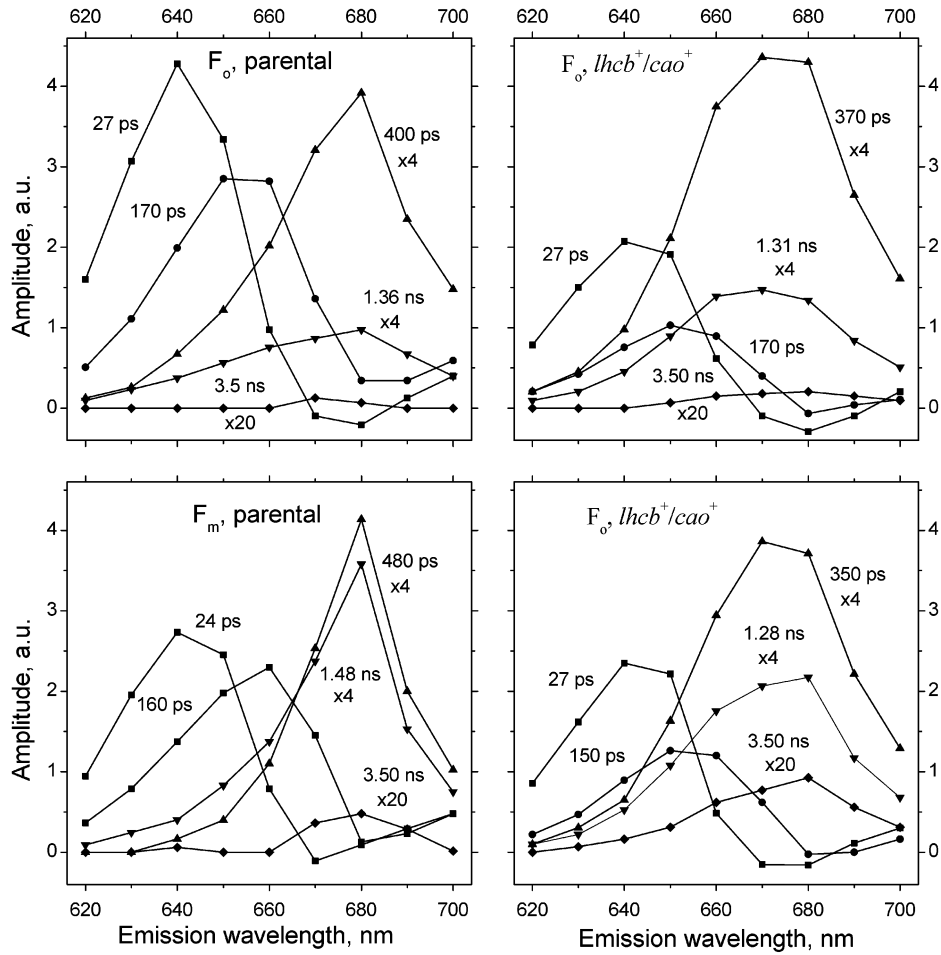


FIGURE 10: Decay associated spectra of fluorescence emission upon phycobilin excitation at 600 nm. The chlorophyll *b/a* ratio in the *lhc b⁺/cao⁺* mutant was 1.2. The amplitudes of selected components were multiplied by the factors indicated in the figure.

Table 2: Analysis of Fluorescence Decay upon Chlorophyll *a* Excitation^a

culture	Chl <i>b/a</i>	emission wavelength, nm	<i>F_O</i> or <i>F_M</i>	global χ^2	amplitudes and lifetimes of decay components			
					1st	2nd	3rd	4th
PS I-less/ <i>chlL</i> [−]	0.0	680–700	<i>F_O</i>	1.09	39.8 ± 1.1 70 ps	45.7 ± 1.5 300 ps	12.6 ± 0.9 1.0 ns	1.9 ± 0.3 2.9 ns
			<i>F_M</i>	1.12		41.3 ± 8.7 310 ps	50.1 ± 8.4 1.4 ns	8.6 ± 0.4 2.9 ns
<i>lhc b⁺/cao⁺</i>	1.2	680–700	<i>F_O</i>	1.10	18.2 ± 6.5 60 ps	61.9 ± 5.2 280 ps	17.5 ± 1.0 1.0 ns	2.3 ± 0.3 3.3 ns
			<i>F_M</i>	1.12		46.4 ± 0.4 270 ps	43.8 ± 2.1 1.3 ns	8.1 ± 1.0 3.5 ns
<i>lhc b⁺/cao⁺</i>	2.8	680–700	<i>F_O</i>	1.06		65.1 ± 1.4 300 ps	29.7 ± 1.9 1.0 ns	5.2 ± 0.6 3.3 ns
			<i>F_M</i>	1.06		41.4 ± 0.9 330 ps	47.5 ± 1.4 1.2 ns	11.0 ± 0.4 3.6 ns
<i>lhc b⁺/cao⁺</i>	2.8	660	<i>F_O</i>	1.09		64.9 320 ps	28.3 1.0 ns	6.8 3.36 ns
			<i>F_M</i>	1.08		42.8 330 ps	43.5 1.2 ns	13.6 3.6 ns

^a Fluorescence lifetime components in the PS I-less/*chlL*[−] strain and in the *lhc b⁺/cao⁺* mutant with different chlorophyll *b/a* ratios obtained from combined analysis of decays detected at 660, 680, 690, and 700 nm upon excitation at 435 nm. Considering that the fluorescence at 680–700 nm is emitted mostly by chlorophyll, the decays at these wavelengths were analyzed globally and the obtained amplitudes were normalized with the total amplitude at each wavelength taken to be 100% and then averaged over the three detection wavelengths. Emission data at 660 nm originated from the same set of experiments as 680–700 nm emission and were not averaged with data obtained at other wavelengths.

PS II (27, 28). Upon excitation at 600 nm, these reactions are masked by the relatively slow energy transfer from phycobilisomes to the PS II complex. Table 2 summarizes the kinetic components obtained from global analysis of fluorescence recorded at 680, 690, and 700 nm corresponding to emission primarily from chlorophyll *a*. In dark-adapted

cells of the PS I-less/*chlL*[−] parental strain four components were required to obtain a good fit. The two major components of fluorescence decay in the parental strain had lifetimes $\tau = 70$ ps and $\tau = 300$ ps with relative amplitudes of 40% and 46%, respectively. When PS II centers were closed by illumination in the presence of DCMU, the

fluorescence decays could be adequately described by just three components with the $\tau = 310$ ps and $\tau = 1.4$ ns components together contributing to more than 90% of the total amplitude.

In dark-adapted cells of the *lhcb⁺/cao⁺* mutant the amplitude of the fast phase ($\tau \sim 70$ ps) of the fluorescence decay elicited by 435 nm excitation decreased with an increase in chlorophyll *b* content. The amplitudes of slower components increased accordingly (Table 2). In the dark-adapted *lhcb⁺/cao⁺* cells with chlorophyll *b/a* ratio of 2.8, the fluorescence decay kinetics could be approximated by just 3 components; no 60–70 ps decay component was apparent. When PS II centers were closed, a consistent decrease in the lifetime of the intermediate component was observed (from ~ 1.4 ns in the parental strain to ~ 1.2 ns in the *lhcb⁺/cao⁺* cells with a chlorophyll *b/a* ratio of 2.8) together with an increase in the lifetime of the slowest component (from 2.9 to 3.6 ns). However, the changes in fluorescence lifetime in closed PS II centers caused by the presence of chlorophyll *b* were relatively minor as compared to the changes in open PS II centers. As the steady-state fluorescence spectra of the *lhcb⁺/cao⁺* cells show significant emission at 650–670 nm (see Figure 9), we have also performed time-resolved fluorescence measurements at 660 nm in this mutant upon excitation at 435 nm. Analysis of fluorescence decay kinetics at 660 nm (see Table 2) shows that fluorescence emission at 660 nm in *lhcb⁺/cao⁺* cells with a chlorophyll *b/a* ratio of 2.8 has essentially the same set of components and relative amplitudes as fluorescence emission at 680–700 nm. This reflects a dynamic equilibrium between pigments emitting at ~ 660 nm (mostly allophycocyanin) and at ~ 680 nm (chlorophyll *a* and the phycobilisome terminal emitter) if the excitation resides in the PS II/phycobilisome complex for longer than 300 ps.

Time-Resolved Fluorescence: Excitation at 450 nm. The steady-state and time-resolved fluorescence measurements presented thus far revealed no significant contribution of chlorophyll *b* to the fluorescence emitted by the *lhcb⁺/cao⁺* mutant. This suggests very efficient energy transfer from chlorophyll *b* to chlorophyll *a* in the *lhcb⁺/cao⁺* strain. The effective coupling between the two types of chromophores in the *lhcb⁺/cao⁺* mutant is supported by the results of fluorescence decay measurements in these cells upon selective excitation of chlorophyll *b* at 450 nm. The kinetic components of fluorescence decay measured at 680 nm in the *lhcb⁺/cao⁺* cells with a chlorophyll *b/a* ratio of 1.2 were similar upon excitation at 450 nm (Table 3) versus at 435 nm (Table 2). However, introduction of a fast ($\tau \sim 30$ –50 ps) component with a large negative amplitude was required to fit the fluorescence decay data recorded at 660 nm. This negative component is likely to reflect energy transfer from PS II core chlorophyll to phycobilisome pigments. Noticeably, no increase in the relative contribution of the very slow component of fluorescence decay (~ 3 ns) was observed upon measurement of fluorescence decay at 660 nm. These data are in line with the absence of a fluorescence increase at 650–670 nm in the steady-state fluorescence emission spectra measured in phycobilisome-free thylakoids upon their excitation at 465 versus 435 nm indicating that essentially all chlorophyll *b* molecules are coupled to chlorophyll *a* in the *lhcb⁺/cao⁺* strain.

Table 3: Analysis of Fluorescence Decay upon Chlorophyll *b* Excitation^a

fluorescence	fluorescence emission, nm	χ^2	fluorescence decay components, amplitude and lifetime			
			1st	2nd	3rd	4th
F_O	680	1.00	16 60 ps	63 280 ps	18 1.00 ns	3 3.0 ns
F_M	680	1.05		49 308 ps	42 1.13 ns	9 3.6 ns
F_O	660	1.01	–36 51 ps	71 280 ps	25 1.00 ns	4 3.0 ns
F_M	660	1.05	–53 28 ps	75 310 ps	20 1.06 ns	5 2.9 ns

^a Fluorescence lifetime components were determined in the *lhcb⁺/cao⁺* mutant upon selective excitation of chlorophyll *b* at 460 nm. The chlorophyll *b/a* ratio in the culture was 1.2.

DISCUSSION

In a previous paper (12) we described a PS I-less/*chlL[–]/lhcb⁺/cao⁺* (here referred as *lhcb⁺/cao⁺*) mutant of *Synechocystis* sp. PCC 6803, which is able to synthesize a significant amount of chlorophyll *b*, a pigment that is not present in wild-type cells. The new pigment is a component of the PS II complex, in which it replaces chlorophyll *a* molecules typically present in this complex. Moreover, pheophytin *b* was detected in PS II of the *lhcb⁺/cao⁺* mutant (12). In this work, we undertook a detailed characterization of PS II centers that contain *b*-type pigments.

Chromophore Composition of PS II. As shown in Table 1, preparations of chlorophyll *b*-containing and control (chlorophyll *b*-less) PS II core particles contained 37–38 chlorophyll molecules/two pheophytins. These data strongly suggest that every chlorophyll-binding site in PS II of the *lhcb⁺/cao⁺* mutant is occupied by either chlorophyll *a* or chlorophyll *b* and that the pheophytin-binding niches in the reaction center are filled with pheophytin *a* or pheophytin *b*. Considering that the chlorophyll *b/a* ratio in *lhcb⁺/cao⁺* cells can be as high as 3 when cells are grown at high temperature (37 °C), PS II centers in this mutant may contain 27–29 chlorophyll *b* and only 9–10 chlorophyll *a* molecules.

Despite the substantial amount of chlorophyll *b* and pheophytin *b*, most of the PS II centers remain photochemically active. For example, measurements of the maximum rate of oxygen evolution (see legend to Figure 3) on a per chlorophyll basis indicate that in the chlorophyll *b*-containing strain the number of functional PS II centers is at least 75% of that in the control. This is confirmed by EPR quantification of Chl_Z^+ and Tyr_D^{OX} in thylakoids isolated from *lhcb⁺/cao⁺* and PS I-less/*chlL[–]* cells (data not shown). The high activity of chlorophyll *b*-containing PS II centers may be related to the fact that the chlorophyll *b/a* ratio in PS II reaction centers was noticeably lower than in PS II core particles (Table 1), suggesting that reaction centers are somewhat enriched in the native chlorophyll *a*. Interestingly, a similar situation was observed in the photosynthetic prokaryote *Acarychloris marina*, in which chlorophyll *d* is the dominant pigment in the PS II antenna; spectroscopy data indicate that PS II reaction centers in this organism contain chlorophyll *a* (29).

Typical reaction center particles isolated from higher plants contain 6 chlorophyll molecules (30). The chlorophyll *b/a* ratio in the preparation of PS II reaction centers obtained from *lhcb⁺/cao⁺* *Synechocystis* cells was about 0.8 (Table

1). Taking into account this ratio and assuming that contamination of our preparation with extra chlorophylls is minimal, one can estimate that 2–3 chlorophyll *a* out of six is substituted by chlorophyll *b* in these reaction centers. The substitution of chlorophyll *a* for chlorophyll *b* in PS II reaction center is rather selective, as is evident from the shift of the absorption maximum of chlorophyll *b*-containing preparation to longer wavelength relative to the chlorophyll *b*-less control (Figure 1). As will be discussed later, it is likely that pheophytin *b* present in reaction centers of the *lhcb*⁺/*cao*⁺ mutant predominantly replaces pheophytin *a* in the active branch. Most authors place the Q_y transition of the redox active pheophytin *a* at wavelengths longer than 676 nm (8, 31–33). Consequently, the loss of pheophytin occurring upon isolation of reaction centers from the *lhcb*⁺/*cao*⁺ mutant (see Table 1) cannot be the sole reason for the observed spectral changes in chlorophyll *b*-containing reaction centers.

A preferential decrease in absorption at about 670 nm in PS II reaction center particles of the *lhcb*⁺/*cao*⁺ mutant suggests the loss of chlorophyll *a* molecules absorbing at rather short wavelengths. Considering that on average about 3 out of 6 chlorophylls *a* have been substituted for chlorophyll *b* in the *lhcb*⁺/*cao*⁺ reaction centers, the replacement of two chlorophylls *a* absorbing at short wavelengths and one chlorophyll *a* absorbing at long wavelength is most compatible with our data. The replacement of low-energy absorbing chlorophyll *a* with chlorophyll *b* is consistent with a small blue shift in the 77 K fluorescence emission spectrum observed in chlorophyll *b*-containing reaction center preparations (Figure 2). Most experimental data suggest that the peripheral chlorophylls (Chl_Z and Chl_D) have the most blue-shifted absorption (3, 32, 34), whereas the B_A accessory chlorophyll has the most red-shifted absorption (3; see also ref 35). However, the assignment of which chlorophylls *a* have been replaced by chlorophyll *b* in the PS II reaction center based exclusively on absorption characteristics of isolated reaction centers is equivocal because of heterogeneity in pigment composition between complexes. Moreover, the removal of the core antenna and loss of Q_A causes structural change in the reaction center and perturbs the absorption properties of individual chromophores (36, 37). This perturbation may have a more pronounced and rather unpredictable effect in chlorophyll *b*-containing reaction centers, which lose both Q_A and one of their pheophytins.

Pheophytin *b* as an Intermediate Electron Carrier. Illumination of PS II core particles from the *lhcb*⁺/*cao*⁺ mutant of *Synechocystis* in the presence of dithionite caused a pronounced bleaching at 418, 440, 650, and 679 nm (Figure 3). The decrease in absorption at 418 and around 680 nm corresponds to photoaccumulation of reduced pheophytin *a*, whereas the bleaching at 440 and 650 nm can be readily explained by reduction of pheophytin *b*. Pheophytin reduction leading to the formation of the pheophytin anion radical is generally characterized by a strong decrease in absorption around the Q_y and Soret absorption bands of the molecule (23, 24). The changes in absorption in the Q_y spectral region upon formation of the pheophytin radical can be assumed to be roughly proportional to the extinction coefficient of the corresponding pheophytin at this wavelength (see ref 24). Taking into account that the in vitro extinction coefficient of the Q_y absorption band of pheophytin *b* is 55–80% of

that of pheophytin *a*, depending on the solvent (16), comparison of the intensity of bleaching at 650 versus ~680 nm in chlorophyll *b*-containing PS II core particles suggests that the amount of reduced pheophytin *b* in this preparation noticeably exceeds the amount of reduced pheophytin *a*. As the preparation of PS II core particles from the *lhcb*⁺/*cao*⁺ strain has approximately equal amounts of pheophytin *a* and pheophytin *b*, the data shown in Figure 3 indicate that pheophytin *b* is predominantly located on the active branch of PS II.

As evidenced from experiments on substitution of (bacterio)pheophytin located in the active branch of electron-transfer pathway in bacterial reaction centers, the important determinant of the efficiency of electron-transfer reaction in modified complexes is the redox midpoint potential of electron carriers (38, 39; see also ref 40). A first approximation of the *E*_m value of pheophytin *b*/pheophytin *b*^{•−} couple in PS II may be obtained from comparison of the *E*_m values for pheophytin *b* and pheophytin *a* in organic solvents. This approach is complicated by the fact that no *E*_m value for pheophytin *b* reduction appears to be present in the literature. However, we expect the midpoint redox potential of pheophytin *b* in vitro to be fairly close to that of pheophytin *a* as replacement of the methyl group by an aldehyde at position 7 of ring B (IUPAC numbering) should have a minor effect on the midpoint redox potential of a corresponding chlorine. Indeed, as shown by Fajer and coauthors (24), the *E*_m of bacteriopheophytin *c*/bacteriopheophytin *c*^{•−} couple differs from that of bacteriopheophytin *e*/bacteriopheophytin *e*^{•−} by only 0.03 V (bacteriopheophytins *c* and *e* have chemical structures essentially similar to that of pheophytins *a* and *b*, respectively). The *E*_m value of a porphyrin can also be estimated considering that the primary oxidation minus reduction potential difference *E*_m^{ox} − *E*_m^{red} of porphyrins is generally close to the singlet excitation energy of these molecules (41). Using the available value of *E*_m^{ox} = +1.23 V for pheophytin *b* dissolved in propionitrile (42) and taking into account that the Q_y absorption maximum of pheophytin *b* in organic solvents is at about 650 nm (16), the *E*_m^{red} value of the pigment can be estimated to be about −0.66 V. This is very close to the values of reduction potentials of pheophytin *a* measured in vitro (−0.64 to −0.78 V; see ref 41) and in vivo (−0.61 V; refs 43 and 44). Consequently, thermodynamic properties of pheophytin *b* in organic solvents do not preclude this pigment from participation in electron-transfer reactions in lieu of pheophytin *a*.

The Bleaching at ~650 nm. When following primary charge separation in PS II core particles from the *lhcb*⁺/*cao*⁺ mutant upon 685 nm excitation, bleaching bands centered around 678 and 650 nm were observed (Figure 4). The 650 nm band was absent in PS II particles of the PS I-less/*chlL*[−] parental strain lacking the *b*-type pigments (Figure 4). The transient absorption decrease around 650 nm in chlorophyll *b*-containing PS II can be attributed to the formation of reduced pheophytin *b* and/or oxidation of chlorophyll *b*, as both of these pigments undergo substantial bleaching at their Q_y transition around 650 nm upon formation of the anion and cation, respectively. As will be explained below, the relative contribution of these two species to the 650 nm bleaching is likely to change during the 1 ns measuring window. Significant bleaching at ~650 nm cannot be due to the localization of excitation on

chlorophyll *b* in a dynamic equilibrium with excited chlorophyll *a* because of (i) the long lifetime of the 650 nm bleaching band (>1 ns) as compared to the average lifetime of excited chlorophyll *a* in PS II (see Figure 10) and (ii) the large energy gap between the Q_y transitions of chlorophyll *a* and chlorophyll *b* (~ 30 nm).

Flash-induced evolution of PS II absorption spectra around 680 nm in the pico- to nanosecond time domain is rather complex and reflects a number of processes, such as decay of the excited state of chlorophyll accompanied by formation of $P680^+Pheo^-$ charge pair and the parallel disappearance of stimulated emission, the oxidation of $Pheo^-$ by Q_A , and concomitant electrochromic shifts in absorption of PS II reaction center chromophores. Values for the rate constant of intrinsic charge separation in PS II cited in the literature vary from $\sim(3 \text{ ps})^{-1}$ (45) to $\sim(20 \text{ ps})^{-1}$ (46). The rate constant of electron transfer from $Pheo^-$ to Q_A in open PS II centers is about $(300 \pm 100 \text{ ps})^{-1}$ (47), whereas reduction of $P680^+$ by Tyr_Z occurs via multiphasic kinetics with the rate-constant of the fastest reaction being about $(20 \text{ ns})^{-1}$ (48). On the basis of the typical rates of photochemical reactions in PS II, the fast (~ 5 ps) phase of absorption increase at ~ 680 nm after photoselective excitation of reaction center chlorophylls may be attributed to the absorption changes accompanying primary charge separation, whereas slower phase(s) (>100 ps) primarily may be due to electron transfer from $Pheo^-$ to Q_A . Taking into account the similarity in absorption changes around 680 nm in PS II core particles of the PS I-less/*chlL* $^-$ and *lhcb* $^+/\text{cao}^+$ strains, the rates of primary charge separation and electron transfer from $Pheo^-$ to Q_A may be very similar in the two types of PS II, despite possibly a small difference in the E_m values of the redox active pheophytins. The development of the ~ 650 nm bleaching (Figure 4C) had about the same rate as the fast phase of disappearance of the bleaching at ~ 680 nm (Figure 4D), suggesting that ~ 650 nm absorption changes reflect primary charge separation, accompanied by pheophytin *b* reduction and possibly by chlorophyll *b* oxidation.

About 1 ns after excitation of PS II, the majority of functional wild-type PS II centers are in the $P680^+Q_A^-$ state (27) and $P680^+$ is the major contributor to absorption changes in the red region of the spectrum. If electron transfer from pheophytin (*b*) to Q_A is not significantly affected in chlorophyll *b*-containing PS II centers, the major component responsible for bleaching at 650 nm 1 ns after excitation is likely to be chlorophyll b^+ . However, a contribution of reduced pheophytin *b* cannot be excluded. If chlorophyll b^+ is indeed the major component responsible for 650 nm bleaching, the amount of chlorophyll b^+ in PS II particles 1 ns after the flash can be up to 40% of that chlorophyll a^+ assuming that (i) the differential extinction coefficients for the chlorophyll *b*/chlorophyll b^+ and chlorophyll *a*/chlorophyll a^+ pairs are roughly proportional to Q_y band absorption of the corresponding chlorophyll and (ii) in the Q_y region chlorophyll *b* absorbs 40% less than chlorophyll *a* (see ref 16).

Which Chlorophyll *b* Is Oxidized in the Reaction Center?

Comparison of the intensities of the 650 and 678 nm bleaching bands 1 ns after flash excitation suggests that nearly one-third of the PS II centers have a positive charge on chlorophyll *b* rather than on chlorophyll *a*. The oxidation of chlorophyll *b* is completed in less than 1 ns, with

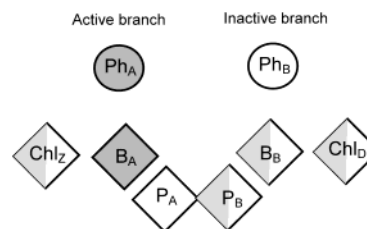


FIGURE 11: Proposed arrangement of chromophores in PS II reaction centers of the *lhcb* $^+/\text{cao}^+$ mutant. Chlorophylls and pheophytins are shown as diamonds and circles, respectively; *a*- and *b*-type pigments are transparent and shaded, respectively. Chromophore-binding sites for which there is no experimental evidence whether they are occupied by chlorophyll *a* or chlorophyll *b* are half-shaded.

apparently high yield and without significant impairment of oxygen evolution. Therefore, the oxidized chlorophyll *b* molecules are unlikely to be the peripheral chlorophylls (Chl_D or Chl_Z) of the PS II reaction center. Our data also show that *lhcb* $^+/\text{cao}^+$ cells have a somewhat slower rate of Q_A^- charge recombination with the donor side and a 3- to 4-fold reduced yield of delayed luminescence that accompanies this recombination (Figure 5). As explained in the next paragraphs, these results can be rationalized by assuming that in the modified reaction centers the monomeric accessory chlorophyll B_A is chlorophyll *b*, whereas the nearby special pair chlorophyll P_A remains chlorophyll *a* (Figure 11); both of these chlorophylls are transiently oxidized upon charge separation in PS II.

According to the scheme presented by Diner and coauthors (3, 9), the excitonic pathway of charge recombination primarily leads to reexcitation of P_A and B_A chlorophylls (i.e. the formation of P_A^* and B_A^*). In addition, positive and negative charge pairs at the donor and acceptor sides of PS II can recombine nonradiatively (i.e. without formation of excited chlorophyll) by direct electron transfer from reduced Q_A^- ($Pheo^-$) to P_A^+ (18, 49). The P_A and B_A chlorophylls in PS II reaction centers from *Synechocystis* have their Q_y transition maxima at 672–673 and 682 nm, respectively (8), which implies that energy difference between P_A^* and B_A^* is ~ 30 meV. Consequently, the probability of formation of B_A^* upon $P_A^+Q_A^-$ charge recombination in control reaction centers at room temperature is about 3.5 times higher than formation of P_A^* . If B_A is chlorophyll *b* and P_A is chlorophyll *a*, as proposed above for chlorophyll *b*-containing reaction centers, then the radiative decay of $P680^+Q_A^-$ through B_A^* should be minimal and most of radiative decay will occur through P_A^* . Given the Q_y transition of chlorophyll *b* is at ~ 650 nm, in these chlorophyll *b*-containing PS II centers the formation of P_A^* rather than B_A^* is favored by a factor of 20 at room temperature and most of the delayed luminescence in these centers is emitted through P_A^* . The higher energy level of P_A^* in chlorophyll *b*-containing centers relative to that of B_A in wild-type reaction centers favors nonradiative path(s) of Q_A^- charge recombination. As a result, the Q_A^- decay in DCMU-treated chlorophyll *b*-containing PS II slows down, which indeed is observed experimentally (Figure 5A).

The energy of excited P_A (~ 1840 mV) is very close to the $E_m^{ox} - E_m^{red}$ difference measured for chlorophyll *b* in vitro (1830 mV; ref 41). Consequently, electrochemical

properties of chlorophyll *b* do not preclude transient reduction of this pigment during electron transfer from P_A to pheophytin.

The oxidation potential of chlorophyll *b* measured in organic solvents *in vitro* is generally 0.1 V more positive than that of chlorophyll *a* (41). The estimated oxidizing potential of P680 chlorophyll(s) is 0.35–0.45 V higher than the oxidizing potential of chlorophyll *a* *in vitro* (see ref 49) due to pigment–protein interactions. Therefore, if oxidized chlorophyll *b* occupies the site of any of the special pair or accessory chlorophylls, the protein environment is expected to shift the oxidation potential of chlorophyll *b* to a lesser extent than that of chlorophyll *a*, as otherwise a considerable accumulation of chlorophyll b^+ would not occur. In normal reaction centers, the E_m value for the B_A/B_A^+ chlorophyll *a* pair was suggested to be more positive than that of P_A/P_A^+ by more than 40 mV (9). In the case of chlorophyll *b*-containing PS II, for which we suggest the replacement of chlorophyll *a* with chlorophyll *b* at the B_A site, the proposed chlorophyll b^+ to chlorophyll a^+ ratio of 1 to 2 is compatible with a ~20 mV difference in E_m values of the B_A/B_A^+ and P_A/P_A^+ pairs.

Energy Transfer in Chlorophyll *b*-Containing PS II. When measuring the fluorescence emission spectra in chlorophyll *b*-containing *Synechocystis* cells, we observed a strong increase in the allophycocyanin fluorescence at ~665 nm, even if chlorophyll *a* or *b* was predominantly excited. Comparison of fluorescence decay kinetics revealed that the long-living ($\tau > 300$ ps) components describing the emission around 660 and 680 nm have similar lifetimes and relative amplitudes. This indicates that ~300 ps after the flash excitons in photosynthetic complexes are thermally equilibrated among allophycocyanin, the terminal emitter(s) of phycobilisomes, and chlorophyll of PS II. In fact, the equilibration of exciton distribution may occur even faster than within ~300 ps as in the *lhcb⁺/cao⁺* strain selective excitation of chlorophyll *b* resulted in intense allophycocyanin fluorescence within 30–50 ps after the flash (see Table 3). Due to the presence of chlorophyll *b*, of which singlet excited-state energy is higher than of chlorophyll *a* and allophycocyanin, the excitonic equilibrium in *lhcb⁺/cao⁺* cells is more shifted to allophycocyanin.

Another striking feature observed upon excitation of chlorophyll *a* at 435 nm was the nearly complete disappearance of the fast (~60–70 ps) component of fluorescence decay typical for open PS II centers, with a corresponding increase in the amplitude of slower components (see Table 2). The most commonly accepted interpretation of the fast fluorescence decay component is that it reflects equilibration between a state with an excitation in PS II and a charge-separated $P680^+Pheo^-$ state (27, 28). If energy transfer to the reaction center and/or energy trapping slow, the fastest phase of fluorescence decay will become smaller and slower. Upon 685 nm laser flashes, primarily exciting reaction center chlorophylls, transient absorption changes around 680 nm in the *lhcb⁺/cao⁺* PS II cores and PS II cores from the parental strain were similar (Figure 4D) suggesting that the intrinsic rate of charge separation in chlorophyll *b*-containing and parental PS II is similar. Therefore, the progressive decrease in the amplitude of the fast phase of fluorescence decay with an increase in chlorophyll *b/a* ratio in *lhcb⁺/cao⁺* cells may be a consequence of slower equilibration

between the excited PS II antenna and charge separation in the reaction center.

Mechanistically, such a deceleration of equilibration (and, effectively, of energy transfer) in chlorophyll *b*-containing PS II may be due, for example, to substitution of the C12 and C30 chlorophylls of the CP43 and CP47 proteins, respectively, by chlorophyll *b*; these two chromophores were proposed to be responsible for 50% of the energy transfer to the reaction center (28). Introduction of chlorophyll *b* at the site of these or other chlorophylls that excitonically couple the antenna and reaction center pigments may “trap” excitation on chlorophyll molecules associated with CP43 and CP47 proteins, thereby increasing the lifetime of fluorescence and raising the F_0 level in chlorophyll *b*-containing PS II centers.

CONCLUDING REMARKS

The study of the *lhcb⁺/cao⁺* mutant of *Synechocystis* sp. PCC 6803 shows that chlorophyll *b* can functionally replace chlorophyll *a* molecules in PS II. Being associated with CP43 and CP47 proteins, chlorophyll *b* functions as a light harvesting pigment. Light energy absorbed by chlorophyll *b* is efficiently transferred to nearby chlorophyll *a* molecules and can be used for charge separation in the PS II reaction center, although energy transfer from PS II core chlorophylls to reaction center pigments appears to be disturbed in the presence of chlorophyll *b*. Chlorophyll *b* can participate in electron-transfer reactions in the PS II reaction center without apparent impairment of reaction center function. The data presented here are consistent with the replacement of the B_A chlorophyll *a* by chlorophyll *b*, whereas the P_A chromophore in the *lhcb⁺/cao⁺* strain is likely remain chlorophyll *a*. If so, charge separation in chlorophyll *b*-containing PS II is expected to be initiated exclusively from the special pair chlorophylls (as in bacterial reaction centers) rather than from primarily B_A^* as has been suggested for the wild-type PS II (see ref 3). Pheophytin *b*, which replaces pheophytin *a* molecules in the photochemically active branch of the PS II reaction center of the *lhcb⁺/cao⁺* mutant, can act as a primary electron acceptor and transfer an electron to Q_A with nearly the same efficiency as pheophytin *a*. This illustrates the considerable flexibility of PS II with respect to the exact molecular nature of important cofactors.

REFERENCES

1. Cogdell, R. J., and Lindsay, J. G. (2000) Tansley Review No. 109-The structure of photosynthetic complexes in bacteria and plants: an illustration of the importance of protein structure to the future development of plant science, *New Phytol.* 145, 167–196.
2. Rhee, K. H. (2001) Photosystem II: The solid structural era, *Annu. Rev. Biophys. Biomol. Struct.* 30, 307–328.
3. Diner, B. A., and Rappaport, F. (2002) Structure, dynamics, and energetics of the primary photochemistry of photosystem II of oxygenic photosynthesis, *Annu. Rev. Plant Biol.* 53, 551–580.
4. Barber, J., and Archer, M. D. (2001) P680, the primary electron donor of photosystem II, *J. Photochem. Photobiol., A* 142, 97–106.
5. Dekker, J. P., and van Grondelle, R. (2000) Primary charge separation in photosystem II, *Photosynth. Res.* 63, 195–208.
6. Faller, P., Pascal, A., and Rutherford, A. W. (2001) β -carotene redox reactions in photosystem II: Electron-transfer pathway, *Biochemistry* 40, 6431–6440.

7. Zouni, A., Witt, H. T., Kern, J., Fromme, P., Krauss, N., Saenger, W., and Orth, P. (2001) Crystal structure of photosystem II from *Synechococcus elongatus* at 3.8 angstrom resolution, *Nature* 409, 739–743.
8. Stewart, D. H., Nixon, P. J., Diner, B. A., and Brudvig, G. W. (2000) Assignment of the Q_y absorbance bands of photosystem II chromophores by low-temperature optical spectroscopy of wild-type and mutant reaction centers, *Biochemistry* 39, 14583–14594.
9. Diner, B. A., Schlodder, E., Nixon, P. J., Coleman, W. J., Rappaport, F., Lavergne, J., Vermaas, W. F. J., and Chisholm, D. A. (2001) Site-directed mutations at D1-His198 and D2-His197 of photosystem II in *Synechocystis* PCC 6803: Sites of primary charge separation and cation and triplet stabilization, *Biochemistry* 40, 9265–9281.
10. Arlt, T., Schmidt, S., Kaiser, W., Lauterwasser, C., Meyer, M., Scheer, H., and Zinth, W. (1993) The accessory bacteriochlorophyll: A real electron carrier in primary photosynthesis, *Proc. Natl. Acad. Sci. U.S.A.* 90, 11757–11761.
11. Durrant, J. R., Klug, D. R., Kwa, S. L. S., van Grondelle, R., Porter, G., and Dekker, J. P. (1995) A multimer model for P680, the primary electron donor of photosystem II, *Proc. Natl. Acad. Sci. U.S.A.* 92, 4798–4802.
12. Xu, H., Vavilin, D., and Vermaas, W. (2001) Chlorophyll *b* can serve as the major pigment in functional photosystem II complexes of cyanobacteria, *Proc. Natl. Acad. Sci. U.S.A.* 98, 14168–14173.
13. Tang, X. S., and Diner, B. A. (1994) Biochemical and spectroscopic characterization of a new oxygen-evolving photosystem II core complex from the cyanobacterium, *Synechocystis* PCC 6803, *Biochemistry* 33, 4594–4603.
14. Shen, G. Z., Boussiba, S., and Vermaas, W. F. J. (1993) *Synechocystis* sp. PCC 6803 strains lacking photosystem I and phycobilisome function, *Plant Cell* 5, 1853–1863.
15. Giorgi, L. B., Nixon, P. J., Merry, S. A. P., Joseph, D. M., Durrant, J. R., Rivas, J. D., Barber, J., Porter, G., and Klug, D. R. (1996) Comparison of primary charge separation in the photosystem II reaction center complex isolated from wild-type and D1-130 mutants of the cyanobacterium, *Synechocystis* PCC 6803, *J. Biol. Chem.* 271, 2093–2101.
16. Lichtenthaler, H. K. (1987) Chlorophylls and carotenoids-pigments of photosynthetic biomembranes, *Methods Enzymol.* 148, 350–382.
17. Porra, R. J., Thompson, W. A., and Kriedemann, P. E. (1989) Determination of accurate extinction coefficients and simultaneous equations for assaying chlorophyll *a* and chlorophyll *b* extracted with 4 different solvents-verification of the concentration of chlorophyll standards by atomic absorption spectroscopy, *Biochim. Biophys. Acta* 975, 384–394.
18. Vavilin, D. V., and Vermaas, W. F. J. (2000) Mutations in the CD-loop region of the D2 protein in *Synechocystis* sp. PCC 6803 modify charge recombination pathways in photosystem II in vivo, *Biochemistry* 39, 14831–14838.
19. Bittersmann, E., and Vermaas, W. (1991) Fluorescence lifetime studies of cyanobacterial photosystem II mutants, *Biochim. Biophys. Acta* 1098, 105–116.
20. Freiberg, A., Jackson, J. A., Lin, S., and Woodbury, N. W. (1998) Subpicosecond pump-supercontinuum probe spectroscopy of LH2 photosynthetic antenna proteins at low temperature, *J. Phys. Chem.* 102, 4372–4380.
21. Funk, C., and Vermaas, W. (1999) A cyanobacterial gene family coding for single-helix proteins resembling part of the light-harvesting proteins from higher plants, *Biochemistry* 38, 9397–9404.
22. Kashino, Y., Lauber, W. M., Carroll, J. A., Wang, Q. J., Whitmarsh, J., Satoh, K., and Pakrasi, H. B. (2002) Proteomic analysis of a highly active photosystem II preparation from the cyanobacterium *Synechocystis* sp. PCC 6803 reveals the presence of novel polypeptides, *Biochemistry* 41, 8004–8012.
23. Klimov, V. V., Klevanik, A. V., Shuvalov, V. A., and Krasnovsky, A. A. (1977) Reduction of pheophytin in the primary light reaction of photosystem II, *FEBS Lett.* 82, 183–186.
24. Fajer, J., Fujita, I., Forman, A., Hanson, L. K., Craig, G. W., Goff, D. A., Kehres, L. A., and Smith, K. M. (1983) Anion radicals of bacteriochlorophyll *c*, bacteriochlorophyll *d*, and bacteriochlorophyll *e*—likely electron acceptor in the primary photochemistry of green and brown photosynthetic bacteria, *J. Am. Chem. Soc.* 105, 3837–3843.
25. Schmid, V. H. R., Thomé, P., Rühle, W., Paulsen, H., Kühlbrandt, W., and Rogl, H. (2001) Chlorophyll *b* is involved in long-wavelength spectral properties of light-harvesting complexes LHC I and LHC II, *FEBS Lett.* 499, 27–31.
26. Mullineaux, C. W., and Holzwarth, A. R. (1991) Kinetics of excitation energy transfer in the cyanobacterial phycobilisome-photosystem II complex, *Biochim. Biophys. Acta* 1098, 68–78.
27. Schatz, G. H., Brock, H., and Holzwarth, A. R. (1988) Kinetic and energetic model for the primary processes in photosystem II, *Biophys. J.* 54, 397–405.
28. Vasil'ev, S., Orth, P., Zouni, A., Owens, T. G., and Bruce, D. (2001) Excited-state dynamics in photosystem II: Insights from the X-ray crystal structure, *Proc. Natl. Acad. Sci. U.S.A.* 98, 8602–8607.
29. Mimuro, M., Akimoto, S., Yamazaki, I., Miyashita, H., and Miyachi, S. (1999) Fluorescence properties of chlorophyll *d*-dominating prokaryotic alga, *Acaryochloris marina*: studies using time-resolved fluorescence spectroscopy on intact cells, *Biochim. Biophys. Acta* 1412, 37–46.
30. Satoh, K. (1996) in *Oxygenic Photosynthesis: The Light Reactions* (Ort, D. R. and Yocum, C. F., Eds.) pp 213–247, Kluwer Academic Publishers, Dordrecht, The Netherlands.
31. Shkuropatov, A. Y., Khatypov, R. A., Shkuropatova, V. A., Zvereva, M. G., Owens, T. G., and Shuvalov, V. A. (1999) Reaction centers of photosystem II with a chemically modified pigment composition: exchange of pheophytins with 13¹-deoxo-13¹-hydroxy-pheophytin *a*, *FEBS Lett.* 450, 163–167.
32. Germano, M., Shkuropatov, A. Y., Permentier, H., Khatypov, R. A., Shuvalov, V. A., Hoff, A. J., and van Gorkom, H. J. (2000) Selective replacement of the active and inactive pheophytin in reaction centres of Photosystem II by 13¹-deoxo-13¹-hydroxy-pheophytin *a* and comparison of their 6 K absorption spectra, *Photosynth. Res.* 64, 189–198.
33. Konermann, L., and Holzwarth, A. R. (1996) Analysis of the absorption spectrum of photosystem II reaction centers: Temperature dependence, pigment assignment, and inhomogeneous broadening, *Biochemistry* 35, 829–842.
34. Vacha, F., Joseph, D. M., Durrant, J. R., Telfer, A., Klug, D. R., Porter, G., and Barber, J. (1995) Photochemistry and spectroscopy of a 5-chlorophyll reaction center of photosystem II isolated by using a Cu-affinity column, *Proc. Natl. Acad. Sci. U.S.A.* 92, 2929–2933.
35. Konermann, L., Yruela, I., and Holzwarth, A. R. (1997) Pigment assignment in the absorption spectrum of the photosystem II reaction center by site-selection fluorescence spectroscopy, *Biochemistry* 36, 7498–7502.
36. Hillmann, B., Brettel, K., van Mieghem, F., Kamrowski, A., Rutherford, A. W., and Schlodder, E. (1995) Charge recombination reactions in photosystem II. 2. Transient absorbance difference spectra and their temperature dependence, *Biochemistry* 34, 4814–4827.
37. Smith, P. J., Peterson, S., Masters, V. M., Wydrzynski, T., Styring, S., Krausz, E., and Pace, R. J. (2002) Magneto-optical measurements of the pigments in fully active photosystem II core complexes from plants, *Biochemistry* 41, 1981–1989.
38. Kirmaier, C., Gaul, D., Debey, R., Holten, D., and Schenck, C. C. (1991) Charge separation in a reaction center incorporating bacteriochlorophyll for photoactive bacteriopheophytin, *Science* 251, 922–927.
39. Huber, H., Meyer, M., Scheer, H., Zinth, W., and Wachtveitl, J. (1998) Temperature dependence of the primary electron-transfer reaction in pigment-modified bacterial reaction centers, *Photosynth. Res.* 55, 153–162.
40. Merry, S. A. P., Nixon, P. J., Barter, L. M. C., Schilstra, M., Porter, G., Barber, J., Durrant, J. R., and Klug, D. R. (1998) Modulation of quantum yield of primary radical pair formation in photosystem II by site-directed mutagenesis affecting radical cations and anions, *Biochemistry* 37, 17439–17447.
41. Watanabe, T., and Kobayashi, M. Electrochemistry of Chlorophylls, in *Chlorophylls* (Scheer, H., Ed.), pp 287–315, CRC Press, Boca Raton, FL.
42. Stanienda, A. (1964) Elektrochemische Untersuchungen der Chlorophylle (*a*, *b*) und Phaeophytine (*a*, *b*), *Z. Phys. Chem.* 229, 257–262.
43. Klimov, V. V., Allakhverdiev, S. I., Demeter, S., and Krasnovskii, A. A. (1979) Photoreduction of pheophytin in the photosystem 2 of chloroplasts with respect to the redox potential of the medium, *Dokl. Akad. Nauk SSSR* 249, 227–230.
44. Rutherford, A. W., Mullet, J. E., and Crofts, A. R. (1981) Measurement of the midpoint potential of the pheophytin acceptor of photosystem II, *FEBS Lett.* 123, 235–237.

45. Wiederrecht, G. P., Seibert, M., Govindjee, and Wasielewski, M. R. (1994) Femtosecond photodichroism studies of isolated photosystem II reaction centers, *Proc. Natl. Acad. Sci. U.S.A.* **91**, 8999–9003.
46. Hastings, G., Durrant, J. R., Barber, J., Porter, G., and Klug, D. R. (1992) Observation of pheophytin reduction in photosystem 2 reaction centers using femtosecond transient absorption spectroscopy, *Biochemistry* **31**, 7638–7647.
47. Bernarding, J., Eckert, H. J., Eichler, H. J., Napiwotzki, A., and Renger, G. (1994) Kinetic studies on the stabilization of the primary radical pair $P680^+Pheo^-$ in different photosystem II preparations from higher plants, *Photochem. Photobiol.* **59**, 566–73.
48. Eckert, H.-J., and Renger, G. (1988) Temperature dependence of $P680^+$ reduction in O_2 -evolving PS II membrane fragments at different redox states S_i of the water oxidizing system, *FEBS Lett.* **236**, 425–431.
49. Rappaport, F., Guergova-Kuras, M., Nixon, P. J., Diner, B. A., and Lavergne, J. (2002) Kinetics and pathways of charge recombination in photosystem II, *Biochemistry* **41**, 8518–8527.

BI026853G